Molecular Human Reproduction, pp. 1–19, 2022
https://doi.org/10.1093/molehr/gaac016

molecular human reproduction

ORIGINAL RESEARCH

Uterine-specific SIRT1 deficiency confers premature uterine aging and impairs invasion and spacing of blastocyst, and stromal cell decidualization, in mice

Magdalina J. Cummings[1,2], Hongyao Yu[3], Sudikshya Paudel[1,2], Guang Hu[3], Xiaoling Li [4], Myriam Hemberger [5,6,7], and Xiaoqiu Wang [1,2,*]

[1]Department of Animal Science, North Carolina State University, Raleigh, NC, USA [2]The Comparative Medicine Institute, North Carolina State University, Raleigh, NC, USA [3]Epigenetics and Stem Cell Biology Laboratory, National Institute of Environmental Health Sciences, Research Triangle Park, NC, USA [4]Signal Transduction Laboratory, National Institute of Environmental Health Sciences, Research Triangle Park, NC, USA [5]Department of Biochemistry & Molecular Biology, Cumming School of Medicine, University of Calgary, Calgary, AB, Canada [6]Department of Medical Genetics, Cumming School of Medicine, University of Calgary, Calgary, AB, Canada [7]Alberta Children's Hospital Research Institute, University of Calgary, Calgary, AB, Canada

*Correspondence address. Box 7621, 231C Polk Hall, 120 W Broughton Dr., Raleigh, NC 27695-7621, USA. Tel: +1-919-515-3497; Fax: +1-919-515-6884; E-mail: xwang97@ncsu.edu https://orcid.org/0000-0001-9660-528X

Submitted on February 15, 2022; resubmitted on April 28, 2022; editorial decision on May 05, 2022

ABSTRACT: A distinct age-related alteration in the uterine environment has recently been identified as a prevalent cause of the reproductive decline in older female mice. However, the molecular mechanisms that underlie age-associated uterine adaptability to pregnancy are not known. Sirtuin 1 (SIRT1), a multifunctional NAD^+-dependent deacetylase that regulates cell viability, senescence and inflammation during aging, is reduced in aged decidua. Thus, we hypothesize that SIRT1 plays a critical role in uterine adaptability to pregnancy and that uterine-specific ablation of *Sirt1* gene accelerates premature uterine aging. Female mice with uterine ablation of *Sirt1* gene using progesterone receptor Cre (Pgr^{Cre}) exhibit subfertility and signs of premature uterine aging. These *Sirt1*-deficient mothers showed decreases in litter size from their 1st pregnancy and became sterile (25.1 ± 2.5 weeks of age) after giving birth to the third litter. We report that uterine-specific *Sirt1* deficiency impairs invasion and spacing of blastocysts, and stromal cell decidualization, leading to abnormal placentation. We found that these problems traced back to the very early stages of hormonal priming of the uterus. During the window of receptivity, *Sirt1* deficiency compromises uterine epithelial–stromal crosstalk, whereby estrogen, progesterone and Indian hedgehog signaling pathways are dysregulated, hampering stromal cell priming for decidualization. Uterine transcriptomic analyses also link these causes to perturbations of histone proteins and epigenetic modifiers, as well as adrenomedullin signaling, hyaluronic acid metabolism, and cell senescence. Strikingly, our results also identified genes with significant overlaps with the transcriptome of uteri from aged mice and transcriptomes related to master regulators of decidualization (e.g. *Foxo1, Wnt4, Sox17, Bmp2, Egfr* and *Nr2f2*). Our results also implicate accelerated deposition of aging-related fibrillar Type I and III collagens in *Sirt1*-deficient uteri. Collectively, SIRT1 is an important age-related regulator of invasion and spacing of blastocysts, as well as decidualization of stromal cells.

Key words: SIRT1 / implantation / stromal cell decidualization / pregnancy / Sirtuin 1 / progesterone receptor signaling

Introduction

Advanced maternal age (i.e. ≥35 years old) is a major risk factor for birth defects (Fitzgerald *et al.*, 1998; Jolly *et al.*, 2000; Cavazos-Rehg *et al.*, 2015; Creanga *et al.*, 2017; Goisis *et al.*, 2017; Duncan *et al.*, 2018), which occur in 3–5% of pregnancies (Hollier *et al.*, 2000). These adverse pregnancy outcomes include, but are not limited to, miscarriage, late fetal and perinatal death, stillbirth, preterm birth and extreme preterm birth, pre-eclampsia and intrauterine growth restriction (IUGR), as well as maternal medical complications such as gestational diabetes and maternal mortality (Hansen, 1986; Astolfi and Zonta, 1999; Jolly *et al.*, 2000; Abel *et al.*, 2002; Jacobsson *et al.*,

2004; Delbaere et al., 2007; Salihu et al., 2008; Lamminpaa et al., 2012). In women over 40 years of age, the incidence of spontaneous abortion can increase to >30% (de la Rochebrochard and Thonneau, 2002). Thus, understanding the precise mechanisms by which female reproductive organs age is a prerequisite for ultimately developing counteracting measures. Much attention has been focused on ovarian function and oocyte quality (Duncan et al., 2018; Laisk et al., 2019), but recent evidence has shown that uterine decidualization and placentation defects are a major cause of age-related declines in fertility (Woods et al., 2017). However, the underlying mechanisms by which reproductive aging affects uterine adaptability to pregnancy are largely unknown.

Sirtuin 1 (SIRT1) is a NAD^+-dependent histone deacetylase (HDAC) that acts on epigenetic and non-epigenetic targets, and also regulates transcription machinery binding to specific chromosomal regions (Guarente, 2000; Ferguson et al., 2015; Ryall et al., 2015; Nevoral et al., 2019). The molecular actions of SIRT1 regulate the cell cycle, DNA repair, adipogenesis, glucose output, insulin sensitivity, fatty acid oxidation, neurogenesis, apoptosis and oxidative stress, thereby affecting cell viability, senescence and inflammation during aging (Guarente, 2000; Yoshizaki et al., 2009; Herranz and Serrano, 2010; Schug et al., 2010; Yi and Luo, 2010; Jin et al., 2011; Toiber et al., 2011; Satoh et al., 2013; Chen et al., 2014; Lee et al., 2019). In particular, SIRT1 and its ortholog have a key role in delaying cell senescence and extending the lifespan of yeast, flies and mice (Kaeberlein et al., 1999; Imai et al., 2000; Chen et al., 2005). Fertility of female *Sirt1*-null mice is significantly compromised. *Sirt1*-null females derived from deletions of exons 5 and 6 are essentially sterile with only one female producing three litters within 7 months of a breeding trial (McBurney et al., 2003). *Sirt1*-null female mice derived from deletion of exon 4 are subfertile with significant decreases in litter size and numbers of litters in a fixed breeding period (Li et al., 2007). *In vitro* studies suggest that SIRT1 interacts with cognate nuclear receptor ESR and PGR to affect estrogen (E2)- or progesterone (P4)-dependent transcriptional activity, respectively (Aoyagi and Archer, 2008; Yao et al., 2010; Moore et al., 2012), as well as progesterone resistance, endometriosis and endometrial cancer (Huang et al., 2021; Sansone et al., 2021; Kim et al., 2022). However, uterine-specific roles of SIRT1 during pregnancy and its roles in uterine aging are not known. Here, we show that SIRT1 decreases in the uterine decidua of aged female mice and is directly regulated by SOX17 and FOXO1, two critical co-regulators of PGR action required for implantation and decidualization (Vasquez et al., 2018; Wang et al., 2018). Thus, the present study aimed to test the hypothesis that SIRT1 plays a critical role in governing age-related uterine receptivity and uterine-specific ablation of SIRT1 accelerates premature uterine aging.

Materials and methods

Animal care and use

All animal experiments were conducted in full compliance with the Guide for the Care and Use of Laboratory Animals published by the National Institutes of Health and with approval of the Institutional Animal Care and Use Committee (IACUC) at North Carolina State University under protocol 19-040-B. C57BL/6J mice were used throughout this study. 'Young' virgin females were generally 6–8 weeks old and 'aged' virgin females were 46–54 weeks old. Timed matings were set up with standard C57BL/6J males between 8 and 16 weeks of age with proven fertility. The morning when the vaginal plug was detected was designate gestational day (GD) 0.5. The uterine-specific knockout mice ($Sox17^{d/d}$; $Foxo1^{d/d}$; $Sirt1^{d/d}$) were generated by crossing $Pgr^{Cre/+}$ mice (Soyal et al., 2005) (a kind gift from Drs. Francesco J. DeMayo at NIEHS, Research Triangle Park, NC, USA and John P. Lydon at Baylor College of Medicine, Houston, TX, USA) with mice carrying $Sox17^{f/f}$ (stock no: 007686, the Jackson Laboratory, Bar Harbor, ME, USA), $Foxo1^{f/f}$ (stock no: 024756, the Jackson Laboratory Bar Harbor, ME, USA), or $Sirt1^{f/f}$ alleles (Cheng et al., 2003; Kazgan et al., 2014) (obtained from Dr Xiaoling Li at NIEHS), respectively.

Animal fertility assay

Conditional knockout and control littermate females at ~6 weeks of age were housed individually and continuously with wildtype C57BL/6J males. Mating was confirmed by the presence of vaginal plugs. Fertility was assessed by monitoring the frequency of litters and litter sizes for a 6-month period.

Artificial decidualization

To assess the ability of the stroma to undergo differentiation and proliferation independent of implantation by a blastocyst, aged or young female mice as well as $Sirt1^{f/f}$ or $Sirt1^{d/d}$ female mice were ovariectomized and treated with exogenous hormones to mimic pregnancy before applying a manual stimulus to a single uterine horn (protocol outlined previously by Finn and Martin (1972)). After ovariectomy and 2 weeks of rest to eliminate endogenous ovarian steroids, mice were administered E2 (E8875, Sigma-Aldrich, St. Louis, MO, USA; 100 ng per mouse) as daily injections for 3 days. After 2 days of rest, mice were treated with E2 (6.7 ng per mouse) and P4 (P0130, Sigma-Aldrich; 1 mg per mouse) for 3 days. On the third day (DD0), mice were administered a single injection of 0.05 ml sesame oil into the right uterine horn. Mice were administered E2 and P4 for 5 more days and euthanized on the fifth day (DD5). Uterine wet weights for the stimulated and control horns were recorded. Weight ratios were calculated by dividing stimulated horn weight by unstimulated horn weight. The whole decidual horn was used in the following analyses including RNA isolation.

Recovery of blastocysts

Adult $Sirt1^{f/f}$ or $Sirt1^{d/d}$ females were mated overnight with wildtype males. Females were separated from males the following morning. The presence of a vaginal plug was considered 0.5 days postcoitum (GD 0.5). Uterine horns were harvested at GD 3.5. Blastocysts were recovered by flushing the uterine lumen with PBS and the numbers were counted under a bright-field microscope. The serum at GD 3.5 of pregnancy was sent to the University of Virginia Center for Research in Reproduction Ligand Assay and Analysis Core for analysis of P4 by radioimmunoassay.

Blastocyst implantation, spacing, invasion and pseudopregnancy

The ability of blastocysts to undergo implantation was determined by mating 8-week-old females with wildtype males. The morning a vaginal

plug was observed was considered 0.5 days postcoitum (GD 0.5). Mice were euthanized at GD 5.5, 6.5 and 9.5. Uteri were excised, imaged, and decidua tissue weights at GD 6.5 were determined. Spacing and invasion of blastocysts were calculated using Image J (NIH). Briefly, the distance between the middle of each of two adjacent implantation sites (IS) was measured to generate a SD for each uterus. High SD indicates uneven spacing. For assessment of invasion of blastocysts, the distance from the blastocyst to the myometrium on the mesometrial (M) side (a) or anti-mesometrial (AM) side (b) was measured to generate a distance ratio (a/b). A high distance ratio indicates significant invasion by the blastocysts. Uteri were fixed in 4% v/v electron microscopy grade paraformaldehyde (PFA) in PBS for histology. Analysis of uterine gene expression during pseudopregnancy was accomplished by mating 8-week-old female mice with vasectomized male mice. The morning of detection of the postcoital vaginal plug was designated pseudopregnant day (PPD) 0.5. The mice were euthanized on PPD 4.5.

RNA *in situ* hybridization analyses

RNAscope *in situ* hybridization was performed according to the manufacturer's instructions using PFA-fixed uterine tissues (~5 µm) and the Mm-SIRT1 probe (418341; Advanced Cell Diagnostic, Newark, CA, USA) for murine *Sirt1* mRNA. A bacterial DapB gene probe (310043; Advanced Cell Diagnostic) was used as the negative control. Following hybridization, slides were washed and probe binding visualized using the HD 2.5 Red Detection Kit (322360-USM; Advanced Cell Diagnostic). Sections were briefly counterstained with hematoxylin before being dehydrated and affixing coverslips with Permount.

RNA isolation

Frozen tissue was homogenized in 1 ml of TRIzol reagent (Thermo Fisher) using a Bead Mill 24 homogenizer (Thermo Fisher), two times at 4.5 m/s for 30 s, and rested intermittently for 20 s on ice. Homogenates were centrifuged for 10 min at 12 500*g* at 4°C to pellet cellular debris. The supernatant was transferred to a 1.5-ml centrifuge tube and mixed with 200 µl of 1-bromo-3-chloropropane by manually shaking for 20 s. The tube was then incubated at room temperature for 3 min, and centrifuged for 18 min at 12 500*g* at 4°C. The upper aqueous phase (~400 µl) was carefully removed, placed into a new 1.5-ml tube, and mixed with 200 µl of chloroform by shaking the tubes for 20 s. Samples were rested for 3 min at room temperature and subsequently centrifuged at 21 000*g* for 18 min at 4°C. Approximately 500 µl of the aqueous layer was transferred to a new tube and mixed with equal parts of 70% ethanol. This mix was filtered in columns from the RNeasy Mini kit (Qiagen, Valenica, CA, USA). Columns were washed once with 700 µl of RW1 buffer (1053394; Qiagen) and three times with 500 µl of RPE buffer (1018013; Qiagen). The RNA was eluted with 30 µl RNase-free water. The quantity and quality of total RNA were determined using spectrometry and denaturing agarose gel electrophoresis, respectively.

Quantitative real-time PCR analyses

RNA was reverse transcribed into cDNA using the Moloney Murine Leukemia Virus (M-MLV; Thermo Fisher) according to the manufacturer's instructions. Quantitative RT-PCR (qRT-PCR) was performed using the CFX Connect Real-Time PCR Detection System (Bio-Rad, Hercules, CA, USA) and the SsoAdvanced™ Universal SYBR® Green Supermix (1725274; Bio-Rad) with oligonucleotide primers synthesized by Integrated DNA Technologies (IDT; Coralville, IA, USA), or the SsoAdvanced™ Universal Probes Supermix (1725284; Bio-Rad) with Taqman probes (Applied Biosystems). Delta delta C_t values were calculated using 18S ribosomal RNA and β-actin (ACTB) control amplification results to determine relative variations in expression of mRNAs per sample. Information for all primers and Taqman probes is provided in Supplementary Table SI.

Western blot analyses

Extracted proteins (30 µg/sample) were denatured, separated using sodium dodecyl sulfate—polyacrylamide gel electrophoresis (4–12% gradient gel at 150 V for 2.5–3 h) and transferred to a nitrocellulose membrane overnight (~16 h) at 20 V using the Bio-Rad Transblot (Bio-Rad). Membranes were blocked in 5% fat-free milk in 20 mmol/l Tris, 150 mmol/l NaCl, pH 7.5 and 0.1% Tween-20 (TBST) for 3 h and then incubated with a primary antibody for SIRT1 (1:1000; #2028) or ACTB (1:5000; #4970) at 4°C overnight with gentle rocking. After washing three times (10 min per time) with TBST, the membranes were incubated for 2 h with a secondary antibody (horseradish-peroxidase-linked anti-rabbit IgG) at 1:10 000 dilutions. The membranes were then washed with TBST, followed by development using enhanced chemiluminescence detection (SuperSignal West Pico) according to the manufacturer's instructions. Western blots were analyzed by measuring the intensity of light emitted from correctly sized bands under ultraviolet light using a ChemiDocTM MP Imaging System (Bio-Rad). Multiple exposures of each western blot were performed to ensure the linearity of chemiluminescence signals.

Histological and immunohistochemical staining

At the time of euthanasia, a mid-portion of the uterine horn was fixed in 4% v/v PFA and embedded in paraffin wax. Embedded tissues were sectioned at 5 µm and baked 1 h at 60°C. Upon cooling, slides were dewaxed using Citrisolv clearing agent (22-143-975, Thermo Fisher) in a decreasing gradient of pure ethanol. For hematoxylin and eosin (H&E) staining, tissues were adequately stained with H&E and were then dehydrated before coverslips were applied. For immunohistochemistry, antigen retrieval was performed according to the manufacturer's instructions (Vector Labs Antigen Unmasking Solution H-3300). Endogenous peroxide was blocked using 3% hydrogen peroxide diluted in methanol. The tissue was blocked with 5–10% normal donkey serum before application of the primary antibody overnight at 4°C. Secondary antibody was diluted in 1% bovine serum albumin at a concentration of 1:200 when required. The ABC reagent was applied to tissues according to manufacturer's instructions (Vector Labs ABC PK-6100). Signal was developed using Vector Labs DAB ImmPACT staining according to manufacturer's instructions (Vector Labs SK-4105). Tissue was counterstained with hematoxylin and dehydrated before affixing coverslips. A semiquantitative grading system (H-score) was used to compare the immunohistochemical staining intensities (Ishibashi *et al.*, 2003; Wang *et al.*, 2018). The H-score was calculated using the following equation: H-score = Σ *Pi* (*i*), where *i* = intensity of

staining with a value of 1, 2 or 3 (weak, moderate or strong, respectively) and *Pi* is the percentage of stained cells for each intensity, varying from 0% to 100%. Information for all antibodies is provided in Supplementary Table SII. For Picosirius red (PSR) staining, tissue sections were deparaffinized in Citrisolv and then rehydrated in a series of graded ethanol baths (100%, 70% and 30%). Slides were washed in water and immersed in a PSR staining solution prepared by dissolving Sirius Red F3BA (Direct Red 80, C.I. 357.82, Sigma-Aldrich) in a saturated aqueous solution of picric acid (P6744, Sigma-Aldrich) at 0.1% w/v. After 40 min of incubation at room temperature, the slides were then incubated in 0.05 M hydrochloric acid for 90 s. Slides were washed in water, dehydrated in 100% ethanol and cleared in Citrisolv for 15 min each before affixing coverslips with Permount.

RNA sequencing and bioinformatic analyses

For RNA sequencing (RNA-seq) from uteri at GD 3.5, total RNA (350 ng) was prepared (see 'RNA isolation' section) to generate a library using the TruSeq Stranded Total RNA with Ribo-Zero Plus kit (Illumina) following the manufacturer's instructions. Indexed libraries were sequenced with a 75 bp single-end protocol on an Illumina NextSeq500 sequencer. Raw fastq data were mapped to the *Mus musculus* GRCm38 genome assembly using HISAT2 v2.2.0. Data were quantitated at a protein-coding mRNA level using Partek Flow bioinformatics software (https://www.partek.com/partek-flow/), and normalized according to total read count (reads per kilobase of transcript per million mapped reads, RPKM), and 75% distribution. Differential expression was calculated using DESeq2. Transcripts with the average RPKM >1 in at least 1 group, $q<0.05$, and at least 1.5-fold difference in RPKM were defined as differentially expressed genes (DEGs). Files were deposited to GEO Datasets under accession number GSE186065.

Data analyses

The DEGs identified using RNA-seq were analyzed using ingenuity pathway analysis software (IPA, http://www.ingenuity.com) and Database for Annotation, Visualization and Integrated Discovery (DAVID, http://david.ncifcrf.gov/). Similar transcriptomes to the *Sirt1*$^{d/d}$ gene expression profile were identified by searching available datasets in the NextBio database (https://www.nextbio.com/). The ChIP-Seq data were analyzed using the Cistrome software (http://cistrome.org/ap/) and visualized on UCSC Genome Browser (https://genome.ucsc.edu). The GraphPad Prism software (v9.2.0) was implemented for one-way ANOVA, multiple comparison test, two-tailed Student's *t* test and χ^2 test analyses. Hierarchal clustering heatmaps were generated using Partek Genomics Suite 6.6 software and MORPHEUS (https://software.boardinstitute.org/morpheus).

Results

Advanced maternal age impairs uterine decidualization

To first confirm that reproductive aging causes uterine defects independent of ovarian function, the ability of the endometrial stromal cells to undergo artificially induced decidualization was determined. The uteri of young female mice (6–8 weeks old) displayed a robust decidual response, as evidenced by increased size and wet weight of the decidua formed in the stimulated right uterine horn at decidual day 2 (DD2) and 5 (DD5) (Fig. 1A and B). However, the uteri of aged females (46–54 weeks old) failed to form a robust decidua at DD2 and DD5 (Fig. 1A), and the ratio of decidual to control horn weight was less than that of young female mice at DD2 ($P<0.01$) and DD5 ($P<0.001$) (Fig. 1B). H&E staining of the mid-section of uterine decidua was conducted to determine the impact of advanced maternal age on the progression of uterine decidualization. After the artificial deciduogenic stimulus at DD0, the uteri of young females exhibited increases in endometrial vascular permeability and development of stromal edema, with enlarged stromal cells with rounded nuclei beginning in the AM pole of the endometrium at DD2 and spreading to the M stromal cells at DD5 (Fig. 1C and Supplementary Fig. S1). On the other hand, these macroscopically identifiable events were not evident in uteri of aged females at DD2 and DD5 (Fig. 1C and Supplementary Fig. S1). Moreover, the endometrial luminal epithelium (LE) remained intact and the center of the decidual tissue in aged mice was fluid-filled at DD5.

SIRT1 expression decreases in decidua of aged mice

Localization and expression of *Sirt1* mRNA in the endometrial compartments of artificially decidualized uteri were determined using *in situ* hybridization and qRT-PCR in young and aged female mice (Fig. 1D–F). At DD2, expression of *Sirt1* mRNA was detectable in uterine LE, glandular epithelium (GE) and stroma (S), but mainly in differentiated stromal cells (DSCs) of young and aged uteri (Fig. 1D). When compared with robust DSCs in young uteri, *Sirt1* mRNA expression decreased in the less differentiated stromal cells of aged uteri (Fig. 1D). The qRT-PCR analyses further demonstrated decreases ($P<0.001$) in the abundance of *Sirt1* mRNA in aged decidua at DD2 (Fig. 1E). At DD5, *Sirt1* mRNA was expressed strongly in uterine LE, GE and DSCs, particularly AM DSCs in uteri of young mice; whereas its abundance was much less in decidua of aged mice (Fig. 1F and Supplementary Fig. S2).

Regulation of endometrial SIRT1 during the peri-implantation period of pregnancy

The temporal and cell-specific expression of *Sirt1* mRNA in the uterus on GD 0.5 to 5.5 was determined in young wildtype female mice using RNA *in situ* hybridization (Fig. 2A). GD 0.5 corresponds to the morning of the presence of the postcoital plug. Expression of *Sirt1* mRNA was detected in both uterine LE and GE between GD 0.5 and 5.5; while stromal expression of *Sirt1* mRNA increased between GD 1.5 and 3.5. By GD 4.5, *Sirt1* mRNA was expressed in uterine LE and DSCs surrounding the IS of blastocysts (E); and increased significantly in the primary (PDZ) and secondary decidual zone at GD 5.5. qRT-PCR analyses confirm that expression of *Sirt1* mRNA increased ($P<0.05$) more in uteri of the mice between GD 1.5 and 2.5 as compared to GD 0.5, 3.5 and PDD 4.5 (Fig. 2B). After mining the independent mouse ChIP-seq datasets (GSE34927, GSE36455, GSE118327 and GSE72892), we identified PGR, ESR, SOX17 and FOXO1 as transcription factors sharing a common binding peak at the promoter region of the *Sirt1* gene in uteri of P4-treated, E2-treated and uteri of

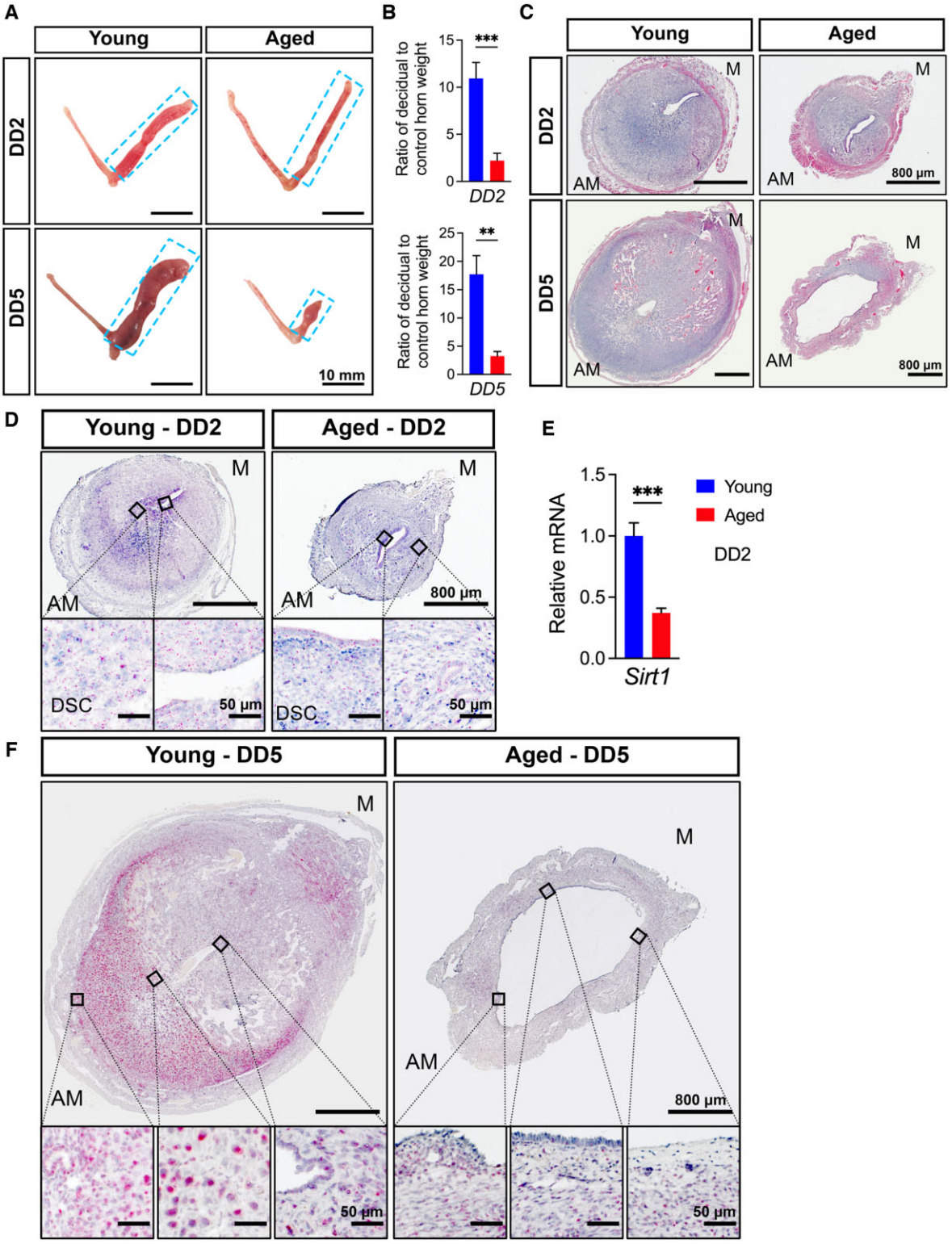

Figure 1. Advanced maternal age in mice impacts artificial decidua formation and *Sirt1* mRNA expression. (**A**) Artificial decidua formation in uteri of young and aged C57BL/6 females at DD2 and DD5. Blue-dashed squares denote decidual tissue in the uterine horn. (**B**) Ratios of decidual uterine horn weight to control uterine horn weight in young and aged females at DD2 and DD5. (**C**) Histological analyses following H&E staining of uterine decidua in young and aged females at DD2 and DD5. (**D–F**) RNAscope *in situ* hybridization (**D**, **F**) and qRT-PCR analyses (**E**) of *Sirt1* mRNA in decidua in young and aged females at DD2 and/or DD5. M, mesometrial side; AM, anti-mesometrial side. n = 6 for DD2; and n = 4 for DD5. DD2, decidual day 2; DD5, decidual day 5; H&E, hematoxylin and eosin; qRT-PCR, quantitative RT-PCR; *Sirt1*, Sirtuin 1. $^{**}P < 0.01$; $^{***}P < 0.001$ (two-tailed Student's *t* test). Data are presented as mean ± SEM. Also see Supplementary Figs. S1 and S2.

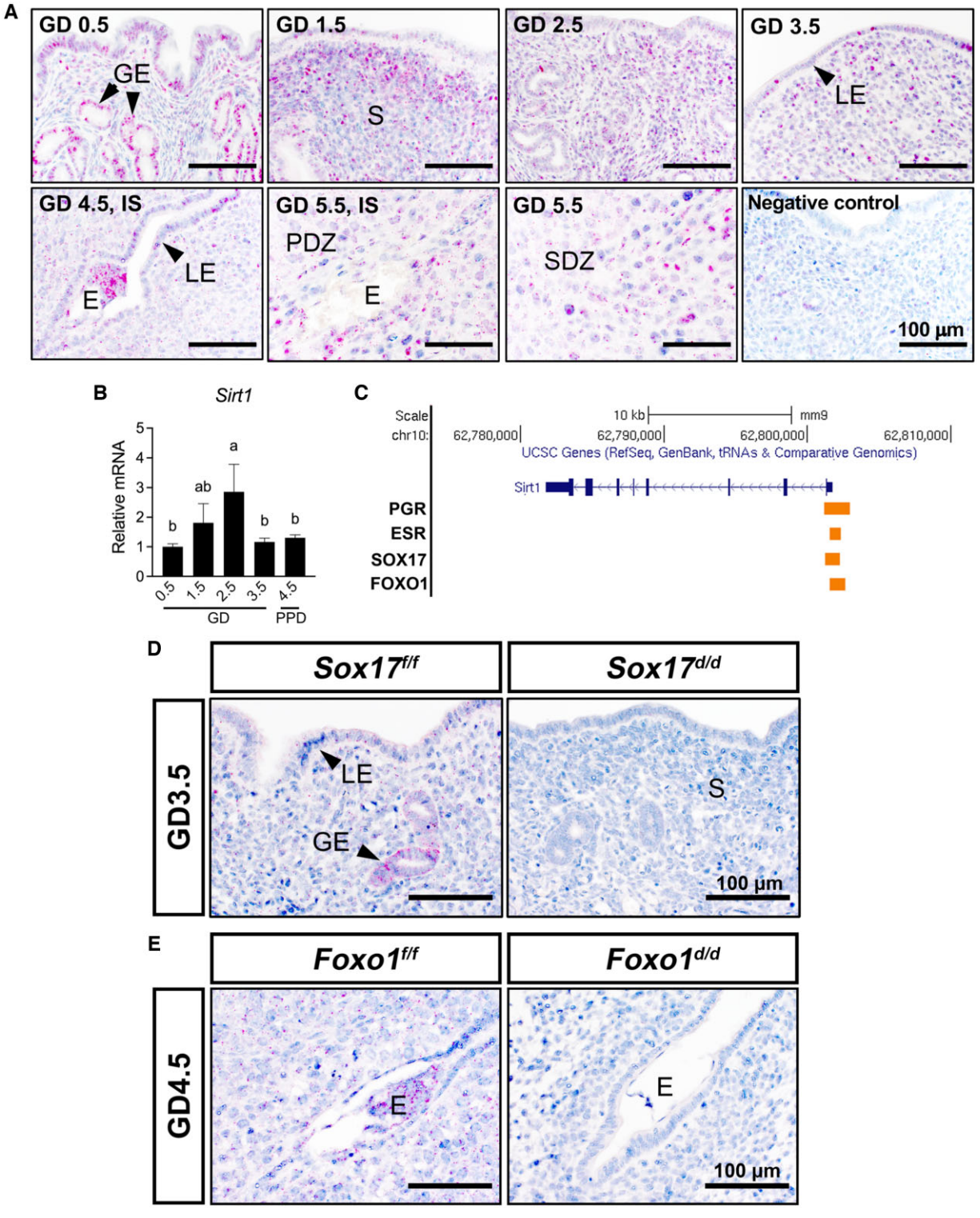

Figure 2. Regulation of expression of *Sirt1* mRNA in uteri of young female mice during the peri-implantation period of pregnancy. (**A**) RNAscope *in situ* hybridization for *Sirt1* mRNA in uteri of young female mice between GD 0.5 and 5.5 (n = 3). (**B**) Quantification of *Sirt1* mRNA in uteri from young female mice between GD 0.5 and 3.5, as well as PPD 4.5 (n = 6). (**C**) Genome Browser tracks of PGR, ESR, SOX17 and FOXO1 binding at promoter region for *Sirt1* gene in P4-treated, E2-treated, GD 3.5 or GD 4.5 uteri. UCSC Genome Browser views showing the mapped read coverage of PGR, ESR, SOX17 and FOXO1 ChIP-seq data (GSE34927. GSE36455, GSE118327 and GSE72892). (**D**) RNAscope *in situ* hybridization for *Sirt1* mRNA in uteri from $Sox17^{f/f}$ and $Sox17^{d/d}$ mice (n = 3) on GD 3.5. (**E**) RNAscope *in situ* hybridization for *Sirt1* mRNA in uteri from $Foxo1^{f/f}$ and $Foxo1^{d/d}$ mice (n = 3) on GD 4.5. E, embryo; GD, gestational day; GE, glandular epithelium; IIS, inter-implantation site; IS, implantation site; LE, luminal epithelium; PDZ, primary decidual zone; PPD, pseudopregnant day; S, stroma; SDZ, secondary decidual zone; *Sirt1*, Sirtuin 1. Different superscript letters denote significant differences ($P < 0.05$, ANOVA with Fisher's LSD post-hoc test). Data are presented as mean ± SEM.

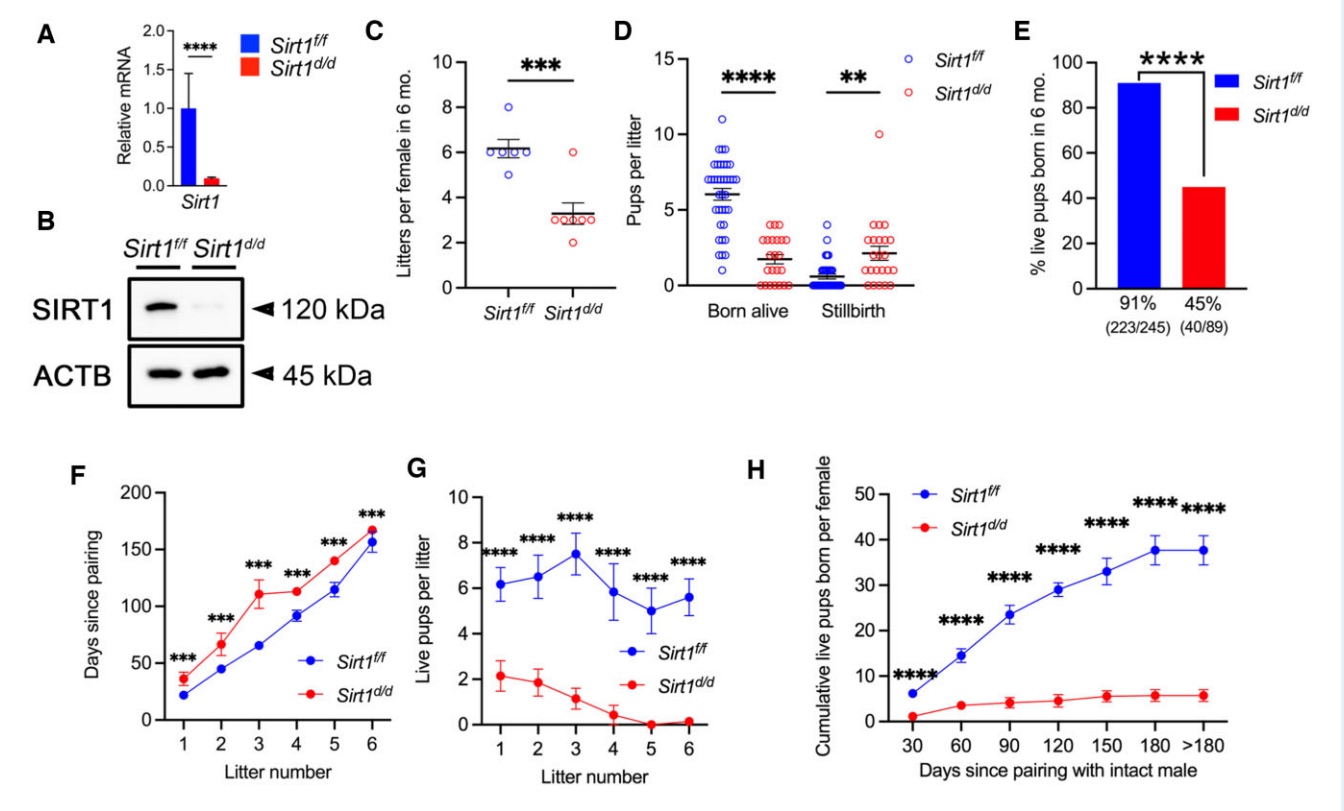

Figure 3. Uterine-specific deletion of *Sirt1* impacts the fertility of female mice in a 6-month breeding trial. (A, B) Generation of *Sirt1* conditional knockout ($Sirt1^{d/d}$; $Pgr^{Cre/+}Sirt1^{f/f}$) female mice using the Pgr^{Cre} mouse model was validated by using qRT-PCR (**A**) and western blot (**B**) analyses. Gene expression was normalized to 18s rRNA in qRT-PCR analyses; and β-actin (ACTB) was used as protein loading control in western blot analyses. ****$P < 0.0001$ (two-tailed Student's *t* test). (**C**) Litters produced from $Sirt1^{f/f}$ (control) and $Sirt1^{d/d}$ female mice. Each dot represents the value for a different individual. ***$P < 0.001$(two-tailed Student's *t* test). (**D**) Stillbirth and live pups born per litter in $Sirt1^{f/f}$ and $Sirt1^{d/d}$ female mice. Each dot represents the value for a different litter. **$P < 0.01$; ****$P < 0.0001$ (two-tailed Student's *t* test). (**E**) Percent live pups born in 6 months from $Sirt1^{f/f}$ and $Sirt1^{d/d}$ female mice. ****$P < 0.0001$ (χ^2 test). (**F**) Time taken to produce a specific number of litters. (**G**) Live pups born in a specific number of litters. (**H**) Cumulative live pups born since pairing. The mean number of pups produced up to each time point is denoted along with the respective error bar, with >180 days representing the day for calculating the total number of live pups produced. ***$P < 0.001$; ****$P <$ 0.0001 (two-way ANOVA with Tukey's multiple comparisons test) at specific time points for contrast between $Sirt1^{f/f}$ (in blue, n = 6) and $Sirt1^{d/d}$ (in red, n = 7) female mice. Data are presented as mean ± SEM. Also see Supplementary Figs. S3 and S4. The uncropped western blot is shown in Supplementary Fig. S3. *Sirt1*, Sirtuin 1; qRT-PCR, quantitative RT-PCR.

pregnant mice on GD 3.5 or GD 4.5 (Fig. 2C). To determine whether SOX17 or FOXO1 directly regulate SIRT1 in uteri of female mice, mice with uterine-specific ablation of *Sox17* ($Sox17^{d/d}$) or *Foxo1* ($Foxo1^{d/d}$) were evaluated. RNA *in situ* hybridization analyses showed that expression of *Sirt1* mRNA decreased in uterine LE, GE and S of $Sox17^{d/d}$ uteri at GD 3.5 (Fig. 2D); and in LE and DSCs of $Foxo1^{d/d}$ uteri within the implantation chamber on GD 4.5 (Fig. 2E).

Female mice lacking uterine SIRT1 are subfertile

The physiological role(s) of SIRT1 in uteri of adult mice was investigated by breeding mice with a conditional allele of *Sirt1* ($Sirt1^{f/f}$ mice) (Cheng *et al.*, 2003; Kazgan *et al.*, 2014) with Pgr^{Cre} mice (Soyal *et al.*, 2005) to ablate *Sirt1* in PGR-positive cells within the uterus ($Sirt1^{d/d}$). Analyses by qRT-PCR confirmed that expression of *Sirt1* mRNA ($P < 0.01$) in whole uteri of $Sirt1^{d/d}$ females was ablated when compared with results from evaluation of uteri from $Sirt1^{f/f}$ mice (Fig. 3A). Evidence of ablation of SIRT1 protein was also confirmed by Western blot analyses (Fig. 3B and Supplementary Fig. S3).

$Sirt1^{d/d}$ female mice were subfertile. During 6 months of breeding trial, $Sirt1^{f/f}$ mice produced 6.2 ± 0.4 litters per female (n = 6 females) with an average of 6.6 ± 0.4 pups per litter (n = 37 litters), whereas $Sirt1^{d/d}$ mice produced only 3.3 ± 0.5 litters per female ($P < 0.001$; n = 7 females) with an average of 3.9 ± 0.5 pups per litter ($P < 0.0001$; n = 23 litters) (Fig. 3C and Supplementary Fig. S4A). Among pups born per litter, control females gave birth to 6.0 ± 0.4 live pups with 0.6 ± 0.2 stillbirth; whereas $Sirt1^{d/d}$ females gave birth to 1.7 ± 0.3 live pups ($P < 0.0001$) with 2.1 ± 0.5 stillbirth ($P < 0.01$) (Fig. 3D). Thus, the percentage of live pups born from $Sirt1^{d/d}$ mothers (223/245; 45%) in 6 months was less ($P < 0.0001$) than for $Sirt1^{f/f}$ control mice (40/89; 91%) (Fig. 3E and Supplementary Fig. S4B). To

further assess fecundity over time in females paired with intact males, we examined the frequency of production of litters of mice (i.e. the rate of litter production) (Fig. 3F), pups per litter at specific litters (Fig. 3G and Supplementary Fig. S4C), and a total number of pups produced per female up to specific time points (i.e. cumulative pups born per female) (Fig. 3H and Supplementary Fig. S4D). A uterine SIRT1 deficiency revealed that *Sirt1*$^{d/d}$ females took a much longer time ($P < 0.001$) to produce each litter when compared with *Sirt1*$^{f/f}$ mothers (Fig. 3F) and had smaller litters ($P < 0.0001$; Supplementary Fig. S4C), fewer live pups ($P < 0.0001$; Fig. 3G), and total pups per litter from their first pregnancy onward. Furthermore, six out of seven *Sirt1*$^{d/d}$ mothers were sterile by 25.1 ± 2.5 weeks of age after giving birth to their 3rd litter (Fig. 3F and G). All of those indices indicate that SIRT1 is necessary to prevent premature reproductive aging. Similarly, cumulative numbers of pups born per female were greater ($P < 0.05$) for *Sirt1*$^{f/f}$ than *Sirt1*$^{d/d}$ mice at 30 days after pairing, and remained different ($P < 0.0001$) thereafter (Fig. 3H and Supplementary Fig. S4D). A plateau was observed in both cumulative total (12.7 ± 1.7) and live (5.7 ± 1.3) pups produced per *Sirt1*$^{d/d}$ female at 150 days after pairing. On the other hand, *Sirt1*$^{f/f}$ mice continued to produce regular litters throughout the 6 months of the breeding trial, i.e. 40.8 ± 4.0 pups as a cumulative total and 37.7 ± 3.2 live pups as a cumulative total per female (Fig. 3H and Supplementary Fig. S4D).

SIRT1 impacts invasion and spacing of blastocysts, and decidualization of uterine stromal cells, independent of ovarian function

There were no differences in the number of blastocysts and serum P4 levels at GD 3.5 between *Sirt1*$^{f/f}$ and *Sirt1*$^{d/d}$ females, suggesting that *Pgr*^{Cre}-derived *Sirt1* deletion does not affect ovarian function (Supplementary Fig. S5A and B). To further dissect the cause of the subfertility in *Sirt1*$^{d/d}$ females, we determined effects on spacing, invasion and implantation of blastocysts, as well as decidualization of uterine stromal cells. Virgin female mice were bred and euthanized at GD 5.5, 6.5 and 9.5 and the uteri were examined for the presence of implantation sites. As shown in Fig. 4A and B, the number of implantation sites for blastocysts was not statistically different between *Sirt1*$^{f/f}$ and *Sirt1*$^{d/d}$ females at GD 5.5, 6.5 and 9.5. However, mice with the SIRT1 deficiency had lower ($P < 0.0001$) weights of the decidua at GD 6.5 and spacing of implantation sites was more uneven ($P < 0.05$) on GD 9.5 (Fig. 4C–E). H&E staining of the mid-section of implantation sites was conducted to determine the impact of SIRT1 deficiency on blastocyst invasion and progression of uterine decidualization. When compared with *Sirt1*$^{f/f}$ uteri in which blastocysts invaded towards AM decidual cells, blastocysts remained in the center of *Sirt1*$^{d/d}$ uteri at GD 5.5 and 6.5 (Fig. 4F, first and second columns), as demonstrated by distance ratio of the implantation sites to each side (AM or M) at the endometrial–myometrial interface (Fig. 4G). By GD 9.5, the definitive placentas of *Sirt1*$^{d/d}$ females were defective and the AM decidual cells did not undergo proper apoptosis to form the decidua capsularis (Kennedy, 2003), insofar as the trophoblast portion was severely under-developed and the main direction of placentation was off-center (Fig. 4F, third column). Immunohistochemical staining of PECAM1, the endothelial marker, also suggests defective angiogenesis in *Sirt1*$^{d/d}$ uteri between GD 5.5 and GD 9.5 (Supplementary Fig. S6). In addition, the ability of the endometrial stromal cells to undergo an artificially induced decidualization was assayed. The uteri of *Sirt1*$^{f/f}$ mice displayed a robust decidual response, as evidenced by increased size and wet weight of the decidua in the stimulated right uterine horn 5 (DD5) days after stimulus delivery (Fig. 4H). However, the decidual/control weight ratio at DD5 was less ($P < 0.05$) in the uteri of *Sirt1*$^{d/d}$ mice (Fig. 4H).

SIRT1 dysregulates localization of PTGS2, FOXO1 and PGR in post-implantation uteri

To determine the possible causes of these decidualization defects, cell-specific expression patterns for PTGS2, FOXO1 and PGR were assessed on GD 5.5, using immunohistochemical analyses, as they are required for decidualization (Takano *et al.*, 2007; Vasquez *et al.*, 2015, 2018) (Fig. 5). PTGS2 was highly expressed in *Sirt1*$^{f/f}$ uteri and localized to the mesometrial DSCs at sites of invading blastocysts; whereas, in *Sirt1*$^{d/d}$ uteri, PTGS2 was expressed in the DSCs closely surrounding the entire blastocyst, suggesting a delay in implantation and dysregulation of decidualization at GD 5.5 (Fig. 5A). Differences in FOXO1 localization confirmed altered implantation as FOXO1 remained localized to nuclei of LE at the fetal–maternal interface and expression was less in mesometrial LE and S of GD 5.5 *Sirt1*$^{d/d}$ uteri (Fig. 5B). Staining of PGR further showed that SIRT1 deficiency had strong effects on inhibition of PGR expression and stromal cell decidualization, demonstrated by downregulation of PGR in DSCs close to the blastocyst and reduced area of DSCs in the endometrium of GD 5.5 *Sirt1*$^{d/d}$ uteri.

SIRT1 regulates uterine E2 and P4 signaling

Our next approaches were aimed at identifying differences in uterine responses during the window of receptivity to implantation when uterine epithelia stop proliferating, become permissive for blastocyst attachment and invasion, and primes stromal cells for decidualization. For this purpose, we mated *Sirt1*$^{f/f}$ and *Sirt1*$^{d/d}$ females with intact wildtype males and dissected uterine horns at GD 3.5 for immunohistochemical and qRT-PCR analyses. Given that uterine function is orchestrated by ovarian steroid hormones (Martin *et al.*, 1973; Finn and Martin, 1974; Curtis Hewitt *et al.*, 2002; Bagchi *et al.*, 2003), the effect of *Sirt1* ablation on E2 and P4 signaling was investigated. Immunohistochemical analyses of the uteri from 6- to 8-week old *Sirt1*$^{d/d}$ mice on GD 3.5, showed increases in estrogen receptor (ESR1) in epithelial cells (Fig. 6A, top panel), but no difference in *Esr1* mRNA was detected between *Sirt1*$^{f/f}$ and *Sirt1*$^{d/d}$ uteri (Fig. 6B, top panel). Concomitantly, as downstream targets of ESR1, *Ltf* mRNA expression was not different, but *Lif* and *Lifr* expression was lower ($P < 0.05$) in *Sirt1*$^{d/d}$ uteri as compared to *Sirt1*$^{f/f}$ control at GD 3.5 (Fig. 6B, top panel). Progesterone receptors (PGR) were reduced in both epithelial cells and stromal cells of *Sirt1*$^{d/d}$ uteri (Fig. 6A, bottom panel). The expression of *Pgr* mRNA, as well as mRNAs for its downstream targets, *Areg* and *Ihh* were also downregulated ($P < 0.01$) in the *Sirt1*$^{d/d}$ uteri (Fig. 6B, second panel). As co-regulators for PGR action, expression of *Foxo1* and *Arid1a mRNAs* was downregulated in the *Sirt1*$^{d/d}$ uteri; and there was no difference in expression of *Sox17* between *Sirt1*$^{f/f}$ and *Sirt1*$^{d/d}$ uteri (Fig. 6B, bottom panel). In addition, expression of *Foxa2* protein and mRNA was not different between *Sirt1*$^{f/f}$ and *Sirt1*$^{d/d}$ uteri (Supplementary Fig. S7).

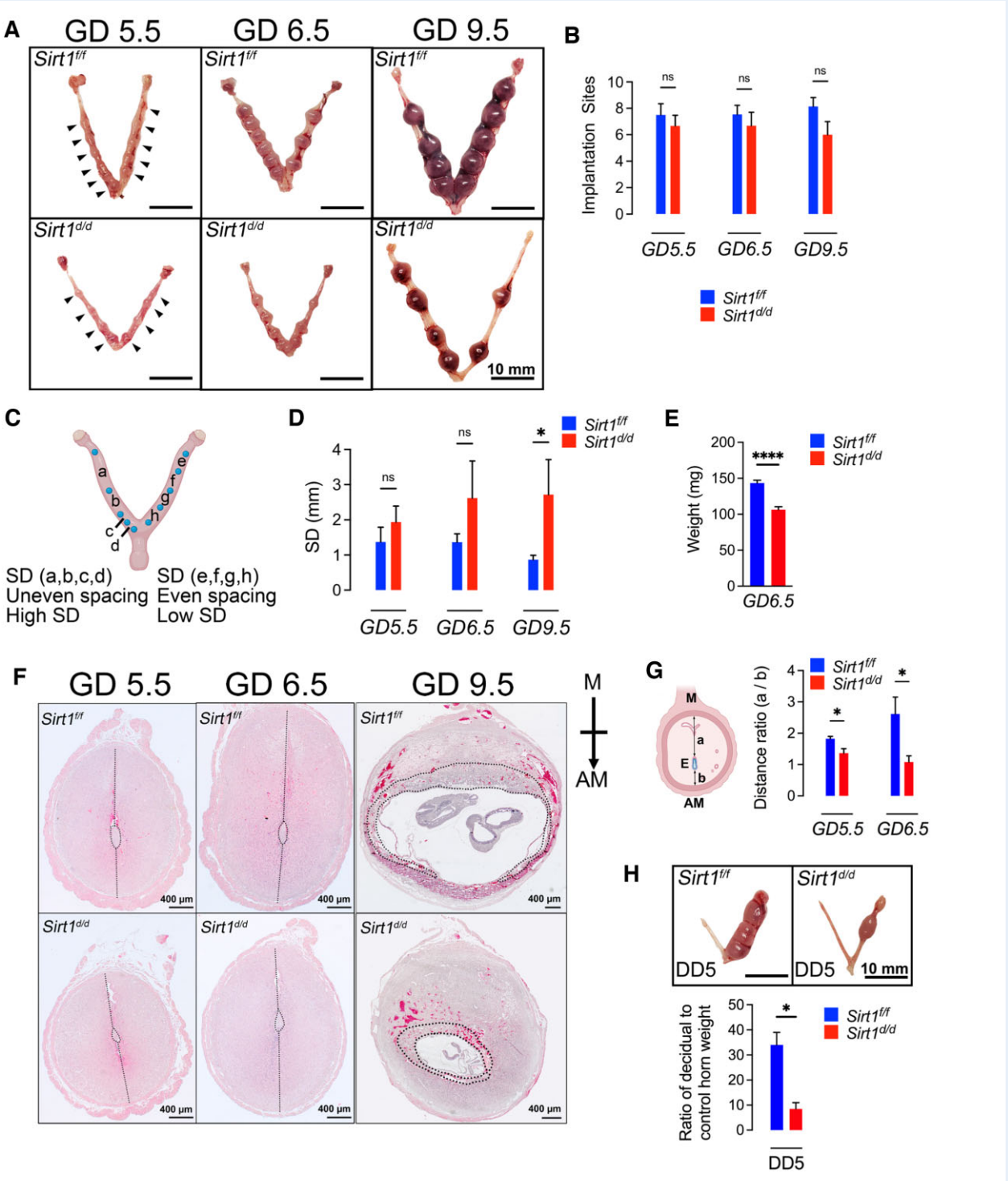

Figure 4. Uterine-specific deletion of *Sirt1* in mice impacts spacing and invasion of blastocysts and stromal cell decidualization. (**A, B**) Images (**A**) and quantification (**B**) of implantation sites in *Sirt1*$^{f/f}$ and *Sirt1*$^{d/d}$ female mice (n = 6). NS, not significant (two-tailed Student's *t* test). (**C**) Illustration of quantitation method for spacing of blastocysts within uterine horns. (**D**) Quantification of spacing of blastocysts in uteri from *Sirt1*$^{f/f}$ and *Sirt1*$^{d/d}$ females using the method depicted in (**C**). n = 6 females per groups. *$P < 0.05$ (two-tailed Student's *t* test). (**E**) Decidual weight in *Sirt1*$^{f/f}$ and *Sirt1*$^{d/d}$ female mice (n = 6). ****$P < 0.0001$ (two-tailed Student's *t* test). (**F**) Histological analyses following H&E staining of uteri from *Sirt1*$^{f/f}$ and *Sirt1*$^{d/d}$ female mice (n = 6). Dotted lines in GD 5.5 and 6.5 indicate the distance from implantation site to AM or M; and dotted lines in GD 9.5 indicate boundary between the fetal trophoblast compartment and the maternal decidua. M, mesometrial pole; AM, anti-mesometrial pole. (**G**) Ratio of the distance between E-to-M to distance between E-to-AM in uteri from *Sirt1*$^{f/f}$ and *Sirt1*$^{d/d}$ female mice at GD 5.5 and 6.5 (n = 6). E, embryo; *Sirt1*, Sirtuin 1. *$P < 0.05$ (two-tailed Student's *t* test). (**H**) Artificial decidua formation and ratio of decidual to control horn weight in *Sirt1*$^{f/f}$ and *Sirt1*$^{d/d}$ female mice (n = 6). *$P < 0.05$ (two-tailed Student's *t* test). Data are presented as mean ± SEM.

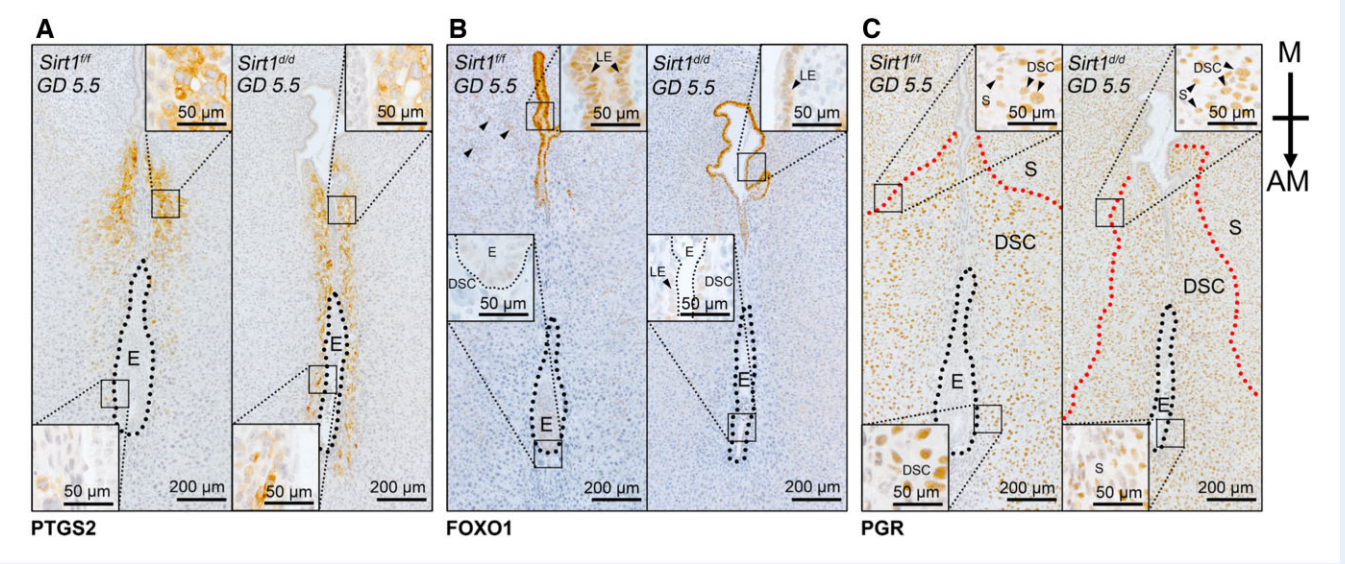

Figure 5. Immunohistochemical staining of proteins in uteri from *Sirt1*$^{f/f}$ and *Sirt1*$^{d/d}$ female mice on GD 5.5. PTGS2 (**A**), FOXO1 (**B**) and PGR (**C**). Black-dotted circles indicate sites of blastocyst implantation. Red-dotted lines indicate the boundary between the DSC and undifferentiated S. Inserts indicate high magnification of box area (n = 3). AM, anti-mesometrial pole; DSC, decidualized stromal cells; E, blastocyst; LE, luminal epithelium; M, mesometrial pole; S, stroma; *Sirt1*, Sirtuin 1.

Sirt1 ablation impairs the Indian hedgehog signaling pathway

Noting that Indian hedgehog (IHH) is a major mediator of PGR signaling in the mouse uterus and significantly reduced in SIRT1-ablated uteri, we further investigated effects on downstream of IHH signaling pathways for uterine epithelial–stromal signaling (Fig. 7). Immunohistochemical analyses of the uteri from 6- to 8-week-old *Sirt1*$^{d/d}$ mice at GD 3.5 revealed decreases in the IHH receptor PTCH1 in uterine stromal cells, as well as a reduction in the downstream mediator COUP-TFII (NR2F2) in stratum compactum stromal cells beneath the uterine epithelium (Fig. 7A). The qRT-PCR analyses further confirmed the dysregulation in the IHH signaling pathway, as demonstrated by decreases ($P < 0.05$) in expression of mRNAs for *Ptch1*, *Gli1*, *Nr2f2* and *Hand2* in GD 3.5 *Sirt1*$^{d/d}$ uteri (Li *et al.*, 2011) (Fig. 7B). Consequently, a reduction in decidualization markers *Bmp2* and *Wnt4* were detected ($P < 0.05$) in *Sirt1*$^{d/d}$ uteri (Lee *et al.*, 2007) (Fig. 7B). However, dysregulation of *Fgf* mRNA expression, that accounts for proliferation of epithelial cells (Li *et al.*, 2011), was not consistent in the *Sirt1*$^{d/d}$ uteri (i.e. increases in *Fgf1* and *Fgf18*; decreases in *Fgf9*; and no change in *Fgf2*, *Fgf7* and *Fgf12*) (Fig. 7B). To determine whether SIRT1 deficiency impacts proliferation of epithelial and stromal cells, expression of proliferation marker Ki67 was determined (Fig. 7B–D). Based on Ki67 staining of uteri from GD 3.5, *Sirt1*$^{f/f}$ mice exhibited minimal levels of cell proliferation (H-score; 1.41 + 0.85), whereas staining of uterine epithelial from *Sirt1*$^{d/d}$ mice was sporadic (H-score; 7.95 + 2.17; $P < 0.05$) (Fig. 7C and D). It is noteworthy that inhibition of proliferation of uterine epithelial cells does not prevent implantation of blastocysts at GD 5.5 in *Sirt1*$^{d/d}$ uteri (Fig. 4A). Intriguingly, the SIRT1 deficiency also decreases Ki67 expression in the stromal cells (Fig. 7C) in which expression of *MKi67* is also reduced in the *Sirt1*$^{d/d}$ uteri (Fig. 7B).

SIRT1 regulates the uterine transcriptome to prime the stromal cells for decidualization

To further identify underlying molecular mechanisms of uterine responses during the window of receptivity for blastocyst implantation, we mated *Sirt1*$^{f/f}$ and *Sirt1*$^{d/d}$ females with intact wildtype males and dissected equivalent pieces of the uterine horns at GD 3.5 for transcriptomic analyses. A total of 6185 genes were dysregulated at GD 3.5 with 2577 genes being upregulated and 3608 genes being downregulated (Supplementary Fig. S8A and Supplementary Table III). Among dysregulated genes by SIRT1 deficiency, several gene clusters were directly associated with uterine receptivity and decidualization as shown in the hierarchical clustering heatmaps, including E2-responsive genes, P4-responsive genes and hedgehog signaling-associated genes (Fig. 8A–C). Clustering of E2-responsive genes revealed that expression of *Hgf*, *Met*, *Igf1*, *Vim* and *Mki67* mRNAs was downregulated in uteri of *Sirt1*$^{d/d}$ females on GD 3.5, while expression of *Esr1*, *Esr2*, *Ltf*, *Slc27a2*, *Muc1* and E-Cadherin (*Cdh1*) mRNAs were upregulated (Fig. 8A). Notably, the majority of P4-responsive genes were downregulated on GD 3.5 in *Sirt1*$^{d/d}$ uteri. Those genes were associated with adhesion and invasion of cells (*Itga5*, *Itga7*, *Itga8*, *Itgb1*, *Itgb2*, *Itgb3*, *Mmp2*, *Mmp7* and *Mmp11*), and proliferation and differentiation of stromal cells (*Bmp2*, *Depp1*, *Gdf10*, *Hoxa3*, *Hoxa5*, *Hoxa9*, *Hoxa10*, *Hoxa11*, *Mcm2*, *Notch3*, *Ptger3*, *Ptgdr2*, *Sfrp1*, *Sfrp2*, *Sfrp4*, *Tgfb1*, *Tgfb2*, and *Tgfb3*) (Fig. 8B). The downregulation of expression of genes in stromal cells provides further evidence for a major defect in mechanisms required for priming stromal cells for decidualization. As expected, IHH pathway associated genes (*Dhh*, *Gli1*, *Gli2*, *Glis1*, *Glis2*, *Glis3*, *Ptch1*, *Ptch2*, *Smo*, *Nr2f2*, *Hand2* and *Klf15*) were downregulated in *Sirt1*$^{d/d}$ uteri on GD 3.5 (Fig. 8C). Intriguingly, further hierarchical clustering

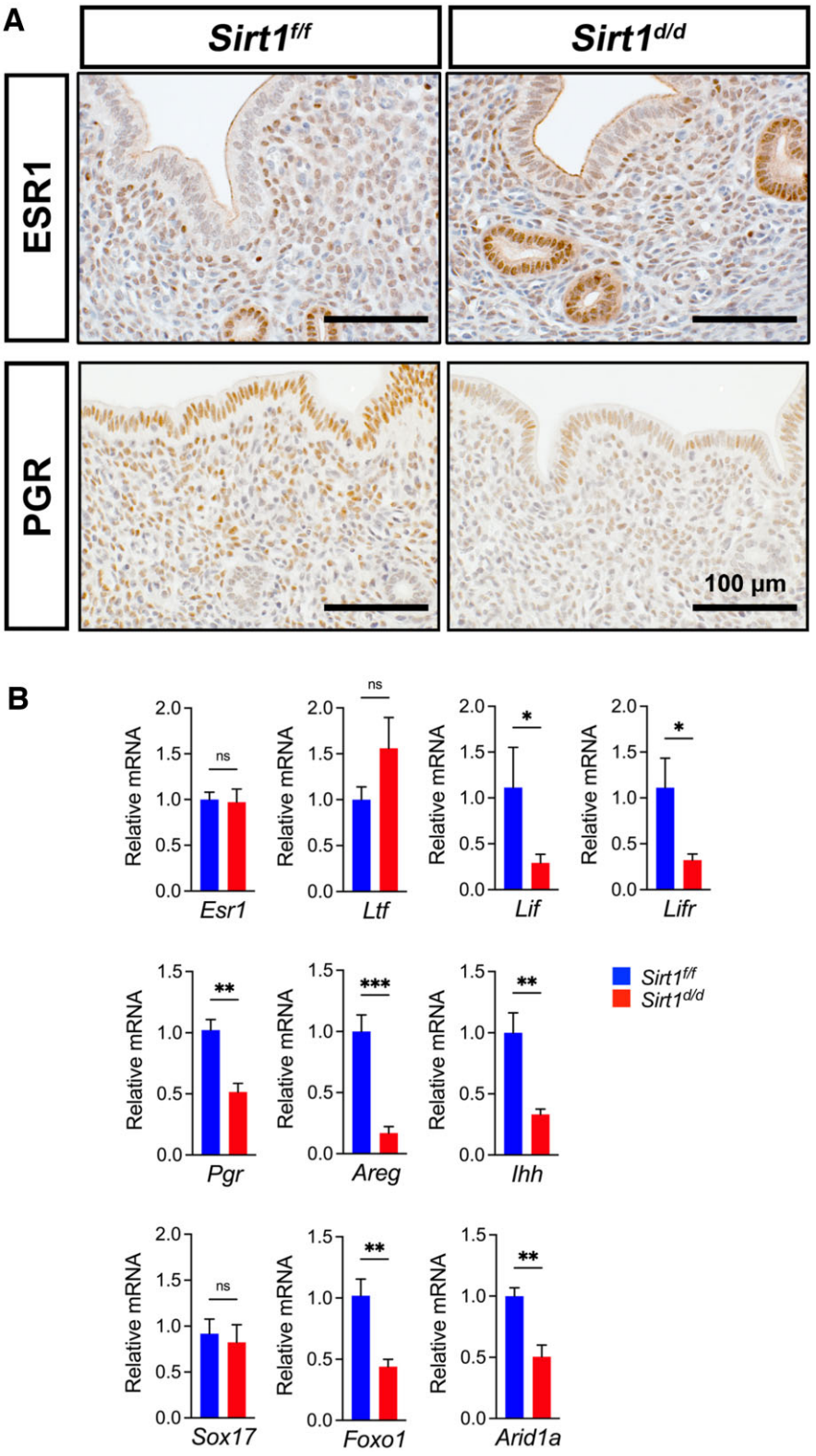

Figure 6. Dysregulated estrogen and progesterone signaling in *Sirt1*-deficient mouse uteri during the window of receptivity to implantation by blastocysts. (**A**) Immunohistochemical staining of ESR1 and PGR in GD 3.5 uteri from *Sirt1*$^{f/f}$ and *Sirt1*$^{d/d}$ female mice (n = 3). (**B**) Quantification of ESR target genes (*Esr1*, *Ltf*, *Lif* and *Lifr*), PGR target genes (*Pgr*, *Areg* and *Ihh*) and PGR co-regulator genes (*Sox17*, *Foxo1* and *Arid1a*) in GD 3.5 uteri from *Sirt1*$^{f/f}$ and *Sirt1*$^{d/d}$ female mice (n = 10). NS, not significant; *$P < 0.05$; **$P < 0.01$; ***$P < 0.001$ (two-tailed *t* test). Data are presented as mean ± SEM. GD, gestational day; *Sirt1*, Sirtuin 1.

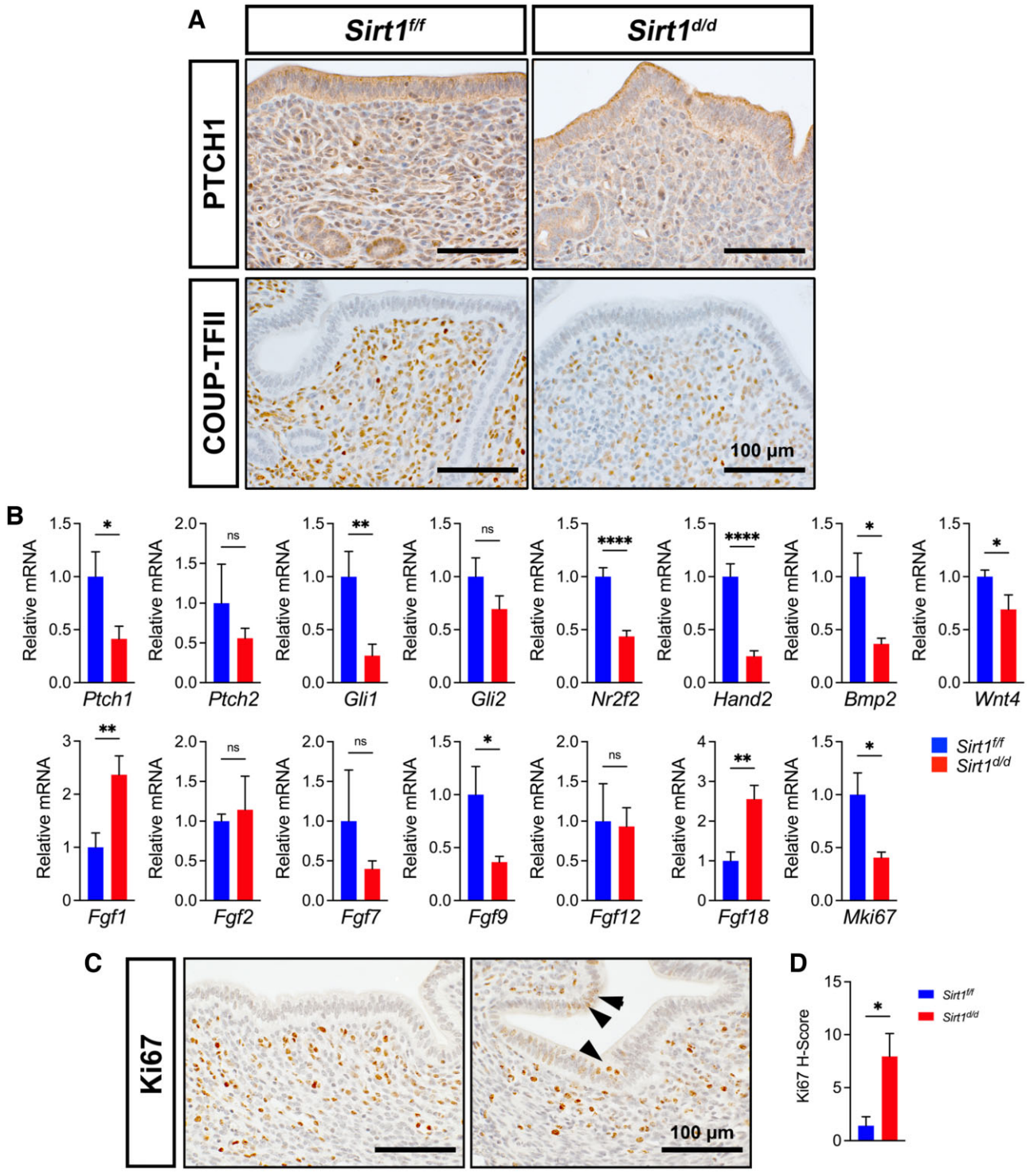

Figure 7. Alteration of Indian Hedgehog signaling pathways in *Sirt1*-deficient mouse uterus during the window of receptivity to implantation by blastocysts. (**A**) Immunohistochemical staining of IHH receptor PTCH1, as well as downstream mediator COUP-TFII in GD 3.5 uteri from *Sirt1*$^{f/f}$ and *Sirt1*$^{d/d}$ females (n = 3). (**B**) Quantification of genes associated with IHH signaling (*Ptch1*, *Ptch2*, *Gli1*, *Gli2*, *Nr2f2* and *Hand2*) to prime stromal cells for decidualization (*Bmp2*, *Wnt4*) and inhibit epithelial proliferation (*Fgf1*, *Fgf2*, *Fgf7*, *Fgf9*, *Fgf12*, *Fgf18* and *Mki67*) in GD 3.5 uteri from *Sirt1*$^{f/f}$ and *Sirt1*$^{d/d}$ females (n = 10). (**C**) Immunohistochemical staining of Ki67 in GD 3.5 uteri from *Sirt1*$^{f/f}$ and *Sirt1*$^{d/d}$ females (n = 3). (**D**) H-score quantification of Ki67 in the endometrial section of *Sirt1*$^{f/f}$ and *Sirt1*$^{d/d}$ females (n=3) at GD 3.5. NS, not significant; *$P < 0.05$; **$P < 0.01$; ****$P < 0.0001$ (two-tailed *t* test). Data are presented as mean ± SEM. IHH, Indian Hedgehog; *Sirt1*, Sirtuin 1.

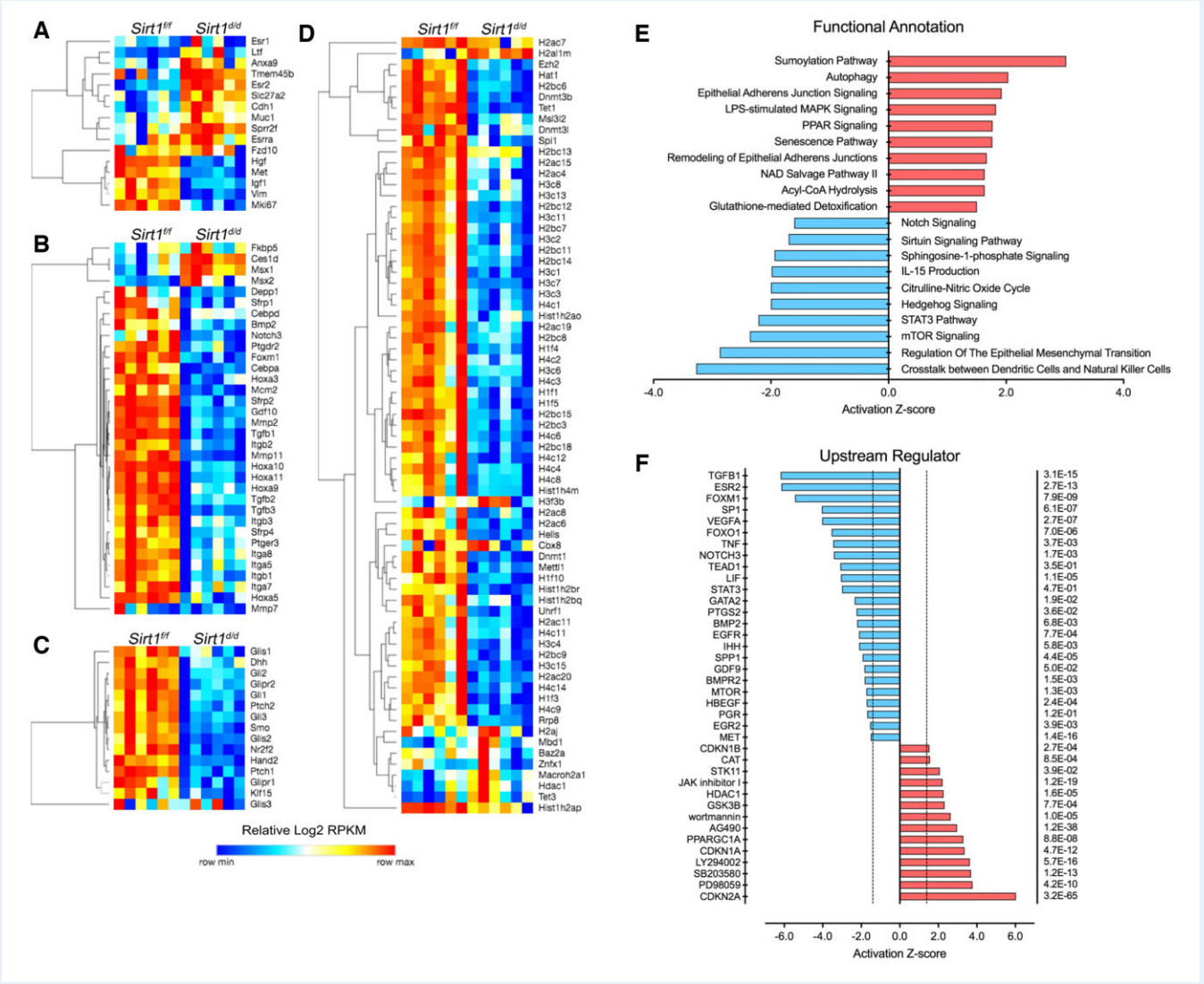

Figure 8. SIRT1 regulation of the uterine transcriptome. (**A–D**) Hierarchical clustering heatmaps depicting the expression profiles of E2-responsive genes (**A**), P4-responsive genes (**B**), IHH signaling pathway (**C**), as well as histone proteins and epigenetic modifiers (**D**) that are differentially expressed between *Sirt1*$^{f/f}$ and *Sirt1*$^{d/d}$ mouse uteri at GD 3.5 generated from RNA-seq analysis (n = 6). (**E**) Enrichment of canonical pathways in DEGs between *Sirt1*$^{f/f}$ and *Sirt1*$^{d/d}$ mouse uteri at GD 3.5 by IPA analysis (n = 6). (**F**) Enrichment of upstream transcriptional regulators for SIRT1-deficient transcriptome at GD 3.5 by IPA analysis (n = 6). Activation Z-score denotes the direction of change in which Z-score > 1.5 indicates activation, and Z-score < 1.5 indicates inhibition ($P < 0.05$). Also see Supplementary Figure S8. DEGs, differentially expressed genes; IPA, ingenuity pathway analysis; RNA-seq, RNA sequencing; SIRT1, Sirtuin 1.

analyses revealed major downregulation of histone proteins and epigenetic modifiers in *Sirt1*$^{d/d}$ uteri on GD 3.5, such as *Ezh2, Dnmt1, Dnmt3b, Dnmt3l, Hdac1, Hat1, Hells, Mbd1, Tet1, Tet3* and *Uhrf1* (Fig. 8D). Other clusters of genes, such as those related to adrenomedullin signaling (*Adm, Ramp1, Ramp2, Calcrl* and *Ackr3*) (Supplementary Fig. S8B) and hyaluronic acid synthesis (*Has1, Has2, Has3, Hyal2* and *Cd44*) (Supplementary Fig. S8C), were also downregulated in *Sirt1*$^{d/d}$ uteri on GD 3.5; while genes associated with junctional complexes between cells (*Cldn23, Cldn3, Add1, Add2* and *Add3*) were upregulated (Supplementary Fig. S8D).

To further identify changes in biological functions of uteri in mice with a SIRT1-deficient transcriptome and obtain evidence for the bases for regulation of expression of particular clusters of genes, Ingenuity Pathway Functional Annotation and Upstream Regulator analyses were performed. The top-enriched functional annotations for the aberrantly controlled gene list (6185 genes) included but were not limited to activation of SUMOylation, autophagy, senescence and NAD salvage pathways; as well as inhibition of crosstalk between dendritic cells and natural killer cells, the epithelial–mesenchymal transition, hedgehog signaling, Sirtuin signaling and Notch signaling pathways (Fig. 8E). Meanwhile, the top-enriched upstream regulators of the SIRT1-deficient transcriptome included but were not limited to: inhibition of TGFB1, ESR2, FOXO1, NOTCH3, LIF, STAT3, GATA2, PTGS2, BMP2, EGFR, IHH, SPP1, GDF9, HBEGF and PGR; and activation of CDKN2A, PD98059 (MEK1 inhibitor), SB203580 (p38 MAPK inhibitor) and LY294002 (PI3K inhibitor) (Fig. 8F). The entire list of

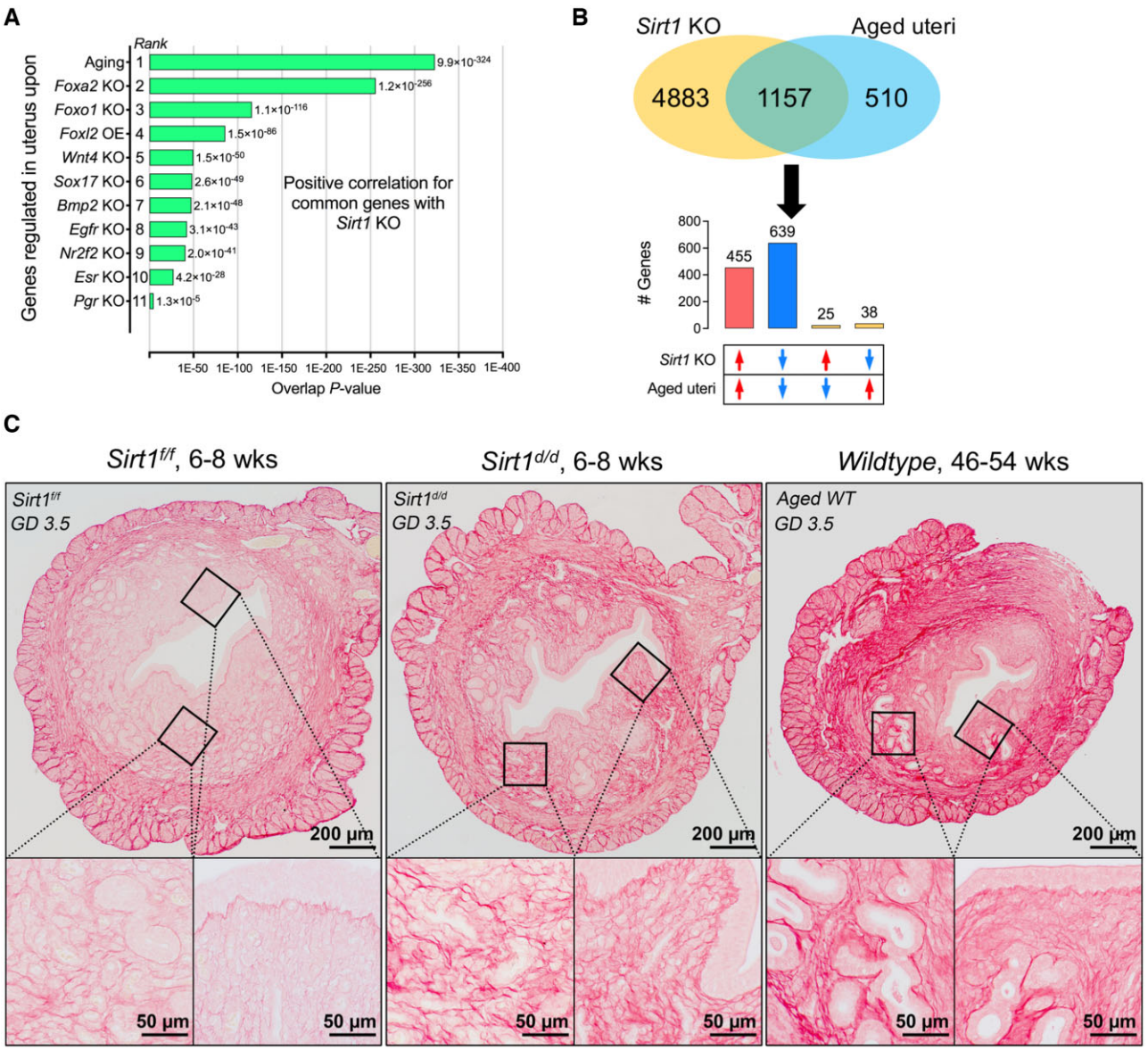

Figure 9. Uterine-specific deletion of *Sirt1* results in premature uterine aging. (**A**) Top uterine transcriptomic biosets overlapping with *Sirt1* KO transcriptome generated by NextBio gene expression profile comparison. (**B**) Overlaps and correlations of *Sirt1* KO with aged transcriptomes at GD 3.5, identifying 1094 genes commonly deregulated in *Sirt1* KO and aged uteri. Also see Supplementary Fig. S9 for a separate comparison between SIRT1 KO and other top similar transcriptomes. (**C**) Picrosirius Red staining of uteri from young $Sirt1^{f/f}$, young $Sirt1^{d/d}$ and aged wildtype female mice, depicting accelerated disposition of aging-related fibrillar Type I and III collagens in SIRT1-deficient uterine stroma. Inserts indicate high magnification of box area. GD, gestational day; KO, knockout; OE, overexpression; *Sirt1*, Sirtuin 1.

functional annotations and upstream regulators is provided in Supplementary Tables SIV and SV.

Uterine-specific deletion of Sirt1 results in premature uterine aging

Next, we performed a correlation search to determine which available dataset in the Illumina BaseSpace Correlation Engine database best characterized the gene expression profile of $Sirt1^{d/d}$ uteri during the window of receptivity to implantation of blastocysts. The top-ranking datasets sharing similar gene expression patterns with the SIRT1-regulated transcriptome at GD 3.5 were uterine transcriptomes of: (i) advanced maternal age; (ii) *Foxa2* knockout, KO; (iii) *Foxo1* KO; (iv) *Foxl2* overexpression, OE; (v) *Wnt4* KO; (6) *Sox17* KO; (vii) *Bmp2* KO; (viii) *Egfr* KO; (ix) *Nr2f2* KO; (x) *Esr1* KO; and (xi) *Pgr* KO (Fig. 9A). With the strongest positive correlation, the $Sirt1^{d/d}$ and aged transcriptomes share 1157 deregulated genes with 455 genes upregulated and 639 genes downregulated (Fig. 9B and Supplementary Table SVI). The overlaps of commonly deregulated genes between *Sirt1* KO and other top-ranking uterine transcriptomes are listed in

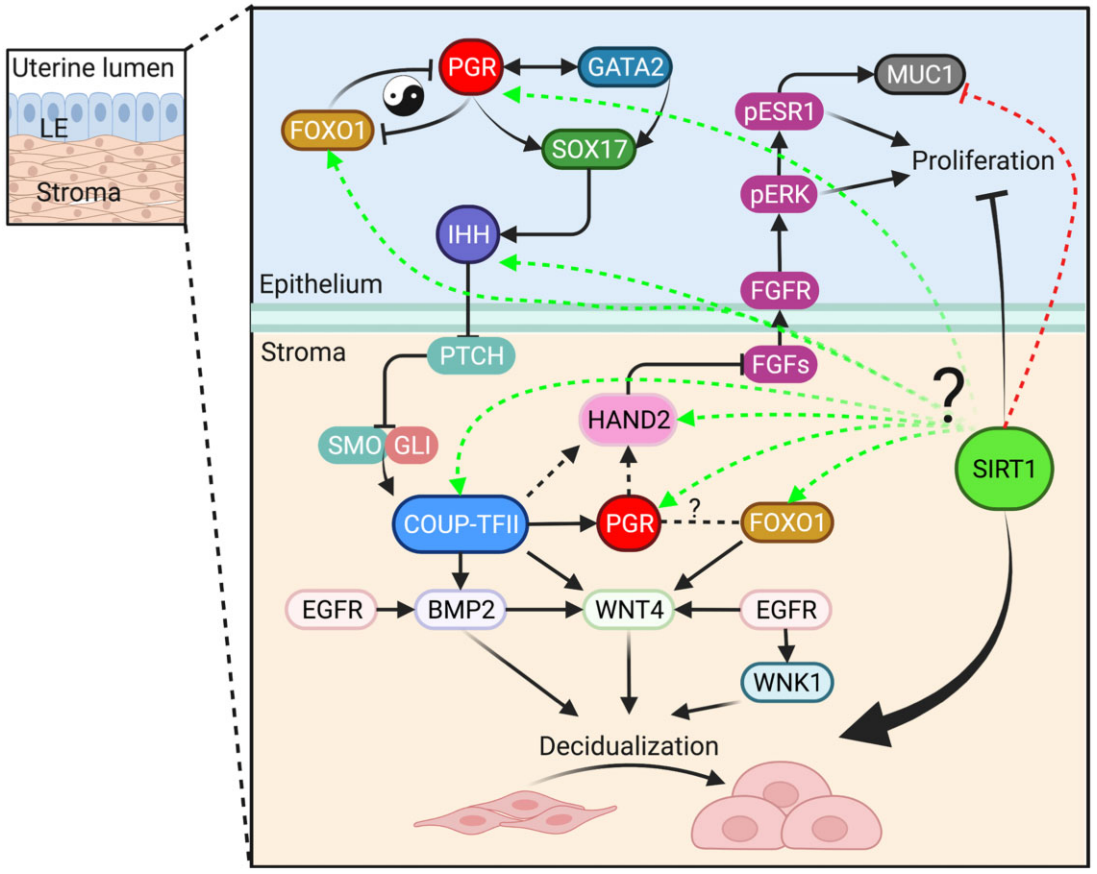

Figure 10. SIRT1 regulates uterine epithelial–stromal interactions to fine-tune epithelial proliferation and direct stromal cell decidualization.

Supplementary Fig. S9. These findings support our hypothesis that SIRT1 plays an essential role in governing age-related changes in uterine receptivity for implantation of blastocysts and stromal cell decidualization, and that uterine-specific ablation of SIRT1 accelerates premature aging of the uterus in mice. In addition, analysis of the deposition of age-related fibrillar collagens, as measured by PSR staining, showed that at GD 3.5 *Sirt1*$^{f/f}$ mice exhibited minimal staining of fibrillar Type I and III collagens in the uterine stroma. On the other hand, both young *Sirt1*$^{d/d}$ and aged wildtype uterine stroma stained positive for Type I and III collagens and thus exhibited age-related uterine stromal fibrosis, suggesting that a SIRT1 deficiency accelerates premature uterine aging.

Discussion

Advanced maternal age negatively impacts reproductive outcomes, leading to pregnancy complications, such as stillbirth, preterm birth or IUGR, as well as a range of developmental defects to the newborn. These adverse pregnancy outcomes are becoming more widespread as women worldwide are delaying childbearing for reasons ranging from higher educational attainment, effective contraception and financial and economic concerns (Mills *et al.*, 2011; Johnson et al., 2012). Recent studies with mice have shed light on the decidualizing uterus that has a blunted PGR signaling response as the major cause of age-related reproductive decline unrelated to oocyte quality (Woods *et al.*, 2017, 2020). It is noteworthy that the number of live offspring declines in older females despite unchanged numbers of early implantation sites, suggesting that embryonic losses must occur post-implantation (Biggers *et al.*, 1962; Finn, 1963). Here, we demonstrate that uterine SIRT1 is a critical driver of age-related PGR action required for uterine epithelial–stromal crosstalk, thereby regulating spacing and implantation of blastocysts, as well as uterine stromal decidualization and placentation (Fig. 10).

SIRT1 is a pivotal regulator of chromatin structure (Guarente, 2000), senescence (Yi and Luo, 2010; Lee *et al.*, 2019) and inflammation (Yoshizaki *et al.*, 2009; Schug *et al.*, 2010). Alteration in SIRT1 signaling is associated with aging in various tissues outside of the uterus (Herranz and Serrano, 2010; Yi and Luo, 2010; Jin *et al.*, 2011; Toiber *et al.*, 2011; Satoh *et al.*, 2013; Chen *et al.*, 2014; Lee *et al.*, 2019) as SIRT1 levels are lower in cells that have been serially spilt or in dividing tissues of aged mice, such as thymus and testis (Sasaki *et al.*, 2006). Recent studies have shown that oocyte-specific ablation of SIRT1 induces premature aging by compromising oocyte quality (Iljas *et al.*, 2020), whereas overexpression of SIRT1 in the oocytes extends

ovarian lifespan in aged mice (Long et al., 2019). Here, we determine that aged uteri exhibit intrinsic defects in the temporal progression of decidual differentiation, accompanied by a decline in *Sirt1* mRNA levels. During the peri-implantation period of pregnancy in young mice, *Sirt1* mRNAs were expressed in the epithelial and stromal compartment of the endometrium. In addition, we provide novel *in vivo* evidence indicating that SIRT1 is the common target positively regulated by SOX17 and FOXO1, two key co-regulators of PGR signaling for implantation and decidualization (Vasquez et al., 2018; Wang et al., 2018). SOX17 is mainly expressed in endometrial epithelium that governs the window of receptivity via uterine epithelial–stromal crosstalk; thus, it stops uterine epithelial cell proliferation via the IHH-COUPTFII-HAND2-FGFs pathway and primes the endometrial stromal cells for proper decidualization (Wang et al., 2018). On the other hand, FOXO1 is expressed in both epithelial and stromal compartments of the uterus in which epithelial FOXO1 is a yin-and-yang regulator of epithelial PGR expression at GD 4.5, and together with stromal FOXO1 govern blastocyst invasion and stromal cell decidualization (Vasquez et al., 2018). As the common target of SOX17 and FOXO1, timely transcription of *Sirt1* gene may be important for governing the window of receptivity (peri-implantation) as well as stimulation of blastocyst invasion and stromal cell decidualization (post-implantation). Thus, we hypothesize that SIRT1 plays a critical role in governing age-related PGR actions required for implantation and decidualization.

To test this hypothesis, we generated mice with uterine-specific ablation of *Sirt1*, which are subfertile with low litter size and frequency of producing offspring, as well as delivering more stillborn pups. The fact that the majority of *Sirt1*$^{d/d}$ mothers become sterile at 25 weeks of age after giving birth to the third litter documents that they experience premature reproductive aging. The majority of pregnancy complications associated with advanced maternal age, such as IUGR and stillbirth, often share underlying pathogenesis owing to deficiencies in placentation, independent of oocyte health (Norwitz, 2006). Previous studies have pinpointed the cause to a more profound defect in stromal cell decidualization that is linked to heterogeneity in expression of both PGR and ESR responsive genes at GD 3.5, and the window of receptivity for implantation of blastocysts in the aged uteri (Woods et al., 2017). Concordant with these observations, our results revealed that a uterine SIRT1 deficiency impairs stromal cell decidualization, spacing and implantation of blastocysts, which lead to abnormal placentation and adverse pregnancy outcomes. We then sought to determine changes to the decidualizing uterus that interfere with spacing, implantation and placentation in SIRT1-deficient mice.

To address this question, we first identified changes at GD 5.5 in SIRT1-deficient mice responsible for the initial progression of stromal cell decidualization. In SIRT1-deficient uteri, the expression pattern of PTGS2 was not altered in DSCs closely surrounding the entire blastocyst, and FOXO1 remained in the intact uterine LE at the fetal–maternal interface, suggesting a delay in implantation. However, there were decreases in PGR in stromal cells proximal to the blastocyst, as well as the restricted area of DSCs indicative of dysregulated decidualization in uteri of SIRT1-deficient mice. In addition, FOXO1 expression was low in uterine LE and S on the mesometrial side of the uteri of *Sirt1*$^{d/d}$ mice on GD 5.5, indicating that the SIRT1 deficiency compromised stromal cell decidualization, possibly via FOXO1. Given that FOXO1 regulates SIRT1 and that they are similar in phenotypes (Vasquez et al., 2018), interactions between FOXO1 and SIRT1 may account for stromal cell decidualization.

Next, we demonstrate that this delay in implantation and uterine decidualization can be traced back to the very early stages of hormonal priming of the uterus at GD 3.5. Together with our analyses of the transcriptome, the SIRT1 deficiency disrupted ESR signaling and suppressed PGR signaling in the uterus during the window of receptivity for implantation of the blastocyst. Both LIF and IHH signaling were altered in this mouse model to yield a phenotype similar to that for SOX17-deficient uteri (Wang et al., 2018). LIF is produced by the uterine GE and acts via receptors in the uterine LE to regulate implantation of blastocysts and stromal cell decidualization (Stewart, 1994). IHH initiates the epithelial–stromal crosstalk required for cessation of proliferation of uterine epithelial cells, blastocyst implantation and stromal cell decidualization (Lee et al., 2006). However, inhibition of proliferation of uterine epithelial cells was not severely compromised because blastocysts were able to implant in *Sirt1*$^{d/d}$ uteri. Instead, failure of stromal cell decidualization is evident owing to dysregulation of the IHH-COUP-TFII-BMP2-WNT4 signaling pathway involving actions requiring epithelial and stromal PGR. Moreover, ADM is a highly conserved peptide hormone required for intrauterine spacing of blastocysts during early pregnancy (Matson et al., 2017; Paudel et al., 2021). Hyaluronan (hyaluronic acid; HA)–CD44 interactions promote proliferation and differentiation of stromal cells (Zhu et al., 2013) and its metabolism fine-tunes the avascular niche and maternal vascular morphogenesis in the implantation chamber of blastocysts (Hadas et al., 2020). Thus, downregulation of the ADM and HA signaling pathway in SIRT1-deficient uteri may also contribute to defects in blastocyst spacing and implantation, as well as stromal cell decidualization. Downregulation of a significant number of histone proteins and dysregulation of epigenetic modifiers further suggests that the uterine SIRT1 deletion triggers DNA damage and perturbations owing to epigenetic modifications, respectively.

Integrating our results with published results from studies of the model for uterine aging effects and key regulators on stromal decidualization and/or implantation failure, we found significant overlaps with uterine transcriptomes at the same days of pregnancy, as well as master regulators of decidualization, notably those for the PGR signaling pathway including *Foxo1, Foxl2, Wnt4, Sox17, Bmp2, Egfr* and *Nr2f2*. Interestingly, the uterine FOXA2-deficient transcriptome ranked second as significantly overlapping with the uterine SIRT1-deficient transcriptome. Given that SIRT1 deletion did not affect FOXA2 expression, but downregulates LIF, it is possible that SIRT1 is a key target downstream of FOXA2, the critical regulator of uterine glandular function required for implantation and stromal cell decidualization (Kelleher et al., 2017). The significant overlaps with uterine transcriptomes of aged mice suggests that by deleting SIRT1, a genetic aging model partially, if not entirely, recapitulating physiological aging in the uterus was produced. Furthermore, accelerated disposition of aging-related fibrillar Type I and III collagens in *Sirt1*-deficient uteri substantiate the functional role of SIRT1 in influencing the adaptability of uterine functions to support pregnancy during reproductive aging.

Collectively, the results of our study highlight the importance of uterine SIRT1 as the critical age-related regulator of PGR actions for implantation, decidualization and placentation in mice. PGR is the master regulator for the establishment and maintenance of pregnancy (Wang et al., 2017); however, a significant diminution in PGR results in

a blunted hormonal response as the uterus ages (Woods *et al.*, 2017). The underlying molecular mechanisms that diminish expression of PGR likely account for uterine aging, a mechanism that has remained elusive. By deleting uterine SIRT1, we produced a genetic model for research on premature uterine aging linked to blunted PGR responses that are similar to those associated with physiological aging. Although the extent to which these findings from the mouse model translate to humans is unknown, it is evident that results of the present study significantly advance our understanding of the molecular changes responsible for blunting PGR actions in aging uteri, independent of potential changes in oocyte quality. Future studies on how SIRT1, the NAD^+-dependent deacetylase, interacts with factors in the PGR signaling pathway (e.g. SIRT1-responsive acetylome, and epigenetic modification) may identify gene signatures in the uterus that are sensitive to reproductive aging. With that new knowledge, research can pursue strategies to counteract adverse effects of aging on outcomes of pregnancy.

Supplementary data

Supplementary data are available at *Molecular Human Reproduction* online.

Data availability

The data underlying this article will be shared on reasonable request to the corresponding author.

Acknowledgements

Contributions of the graduate students and postdoctoral fellows from the Laboratory of Reproductive and Developmental Biology are gratefully acknowledged. The authors also thank Drs. Francesco J. DeMayo and Fuller W. Bazer for scientific discussion, and Drs Francesco J. DeMayo and John P. Lydon for providing *Pgr*-Cre mice.

Authors' roles

X.W. conceived, designed the research, wrote the article and prepared the figures. M.J.C, H.Y., and S.P. performed the experiments and data curation. M.J.C., G.H., X.L., M.H. contributed to experimental design and data analysis. G.H., X.L. and M.H. contributed to manuscript editing. All authors reviewed the article.

Funding

This work was supported by the Research and Innovation Seed Funding (2021-1946 to X.W.), Center for Human Health and the Environment Pilot Project Program Award (ES025128 to X.W.) from North Carolina State University, and Animal Reproduction Program (no. 2022-67015-36491 to X.W.) from the USDA National Institute of Food and Agriculture. The funders had no role in study design, data collection and analysis, decision to publish, or preparation of the manuscript.

Conflict of interest

All authors declare no conflict of interest.

References

Abel EL, Kruger M, Burd L. Effects of maternal and paternal age on Caucasian and Native American preterm births and birth weights. *Am J Perinatol* 2002;**19**:49–54.

Aoyagi S, Archer TK. Nicotinamide uncouples hormone-dependent chromatin remodeling from transcription complex assembly. *Mol Cell Biol* 2008;**28**:30–39.

Astolfi P, Zonta LA. Risks of preterm delivery and association with maternal age, birth order, and fetal gender. *Hum Reprod* 1999;**14**: 2891–2894.

Bagchi IC, Cheon YP, Li Q, Bagchi MK. Progesterone receptor-regulated gene networks in implantation. *Front Biosci* 2003;**8**: s852–s861.

Biggers JD, Finn CA, Mc LA. Long-term reproductive performance of female mice. II. Variation of litter size with parity. *J Reprod Fertil* 1962;**3**:313–330.

Cavazos-Rehg PA, Krauss MJ, Spitznagel EL, Bommarito K, Madden T, Olsen MA, Subramaniam H, Peipert JF, Bierut LJ. Maternal age and risk of labor and delivery complications. *Matern Child Health J* 2015;**19**:1202–1211.

Chen D, Steele AD, Lindquist S, Guarente L. Increase in activity during calorie restriction requires Sirt1. *Science* 2005;**310**:1641.

Chen H, Liu X, Zhu W, Chen H, Hu X, Jiang Z, Xu Y, Wang L, Zhou Y, Chen P *et al.* SIRT1 ameliorates age-related senescence of mesenchymal stem cells via modulating telomere shelterin. *Front Aging Neurosci* 2014;**6**:103.

Cheng HL, Mostoslavsky R, Saito S, Manis JP, Gu Y, Patel P, Bronson R, Appella E, Alt FW, Chua KF. Developmental defects and p53 hyperacetylation in Sir2 homolog (SIRT1)-deficient mice. *Proc Natl Acad Sci USA* 2003;**100**:10794–10799.

Creanga AA, Syverson C, Seed K, Callaghan WM. Pregnancy-related mortality in the United States, 2011-2013. *Obstet Gynecol* 2017; **130**:366–373.

Curtis Hewitt S, Goulding EH, Eddy EM, Korach KS. Studies using the estrogen receptor alpha knockout uterus demonstrate that implantation but not decidualization-associated signaling is estrogen dependent. *Biol Reprod* 2002;**67**:1268–1277.

de la Rochebrochard E, Thonneau P. Paternal age and maternal age are risk factors for miscarriage; results of a multicentre European study. *Hum Reprod* 2002;**17**:1649–1656.

Delbaere I, Verstraelen H, Goetgeluk S, Martens G, De Backer G, Temmerman M. Pregnancy outcome in primiparae of advanced maternal age. *Eur J Obstet Gynecol Reprod Biol* 2007;**135**:41–46.

Duncan FE, Confino R, Pavone ME. Chapter 9—female reproductive aging: from consequences to mechanisms, markers, and treatments. In: JL Ram, PM Conn (eds). *Conn's Handbook of Models for Human Aging*, 2nd edn. Cambridge, Massachusetts: Academic Press, 2018,109–130.

Ferguson D, Shao N, Heller E, Feng J, Neve R, Kim HD, Call T, Magazu S, Shen L, Nestler EJ. SIRT1-FOXO3a regulate cocaine actions in the nucleus accumbens. *J Neurosci* 2015;**35**:3100–3111.

Finn CA. Reproductive capacity and litter size in mice: effect of age and environment. *J Reprod Fertil* 1963;**6**:205–214.

Finn CA, Martin L. Endocrine control of the timing of endometrial sensitivity to a decidual stimulus. *Biol Reprod* 1972;**7**:82–86.

Finn CA, Martin L. The control of implantation. *J Reprod Fertil* 1974; **39**:195–206.

Fitzgerald C, Zimon AE, Jones EE. Aging and reproductive potential in women. *Yale J Biol Med* 1998;**71**:367–381.

Goisis A, Remes H, Barclay K, Martikainen P, Myrskyla M. Advanced maternal age and the risk of low birth weight and preterm delivery: a within-family analysis using Finnish population registers. *Am J Epidemiol* 2017;**186**:1219–1226.

Guarente L. Sir2 links chromatin silencing, metabolism, and aging. *Genes Dev* 2000;**14**:1021–1026.

Hadas R, Gershon E, Cohen A, Atrakchi O, Lazar S, Golani O, Dassa B, Elbaz M, Cohen G, Eilam R *et al*. Hyaluronan control of the primary vascular barrier during early mouse pregnancy is mediated by uterine NK cells. *JCI Insight* 2020;**5**:e135775.

Hansen JP. Older maternal age and pregnancy outcome: a review of the literature. *Obstet Gynecol Surv* 1986;**41**:726–742.

Herranz D, Serrano M. Impact of Sirt1 on mammalian aging. *Aging (Albany NY)* 2010;**2**:315–316.

Hollier LM, Leveno KJ, Kelly MA, MCintire DD, Cunningham FG. Maternal age and malformations in singleton births. *Obstet Gynecol* 2000;**96**:701–706.

Huang S, Li Y, Sheng G, Meng Q, Hu Q, Gao X, Shang Z, Lv Q. Sirtuin 1 promotes autophagy and proliferation of endometrial cancer cells by reducing acetylation level of LC3. *Cell Biol Int* 2021;**45**: 1050–1059.

Iljas JD, Wei Z, Homer HA. Sirt1 sustains female fertility by slowing age-related decline in oocyte quality required for post-fertilization embryo development. *Aging Cell* 2020;**19**:e13204.

Imai S, Armstrong CM, Kaeberlein M, Guarente L. Transcriptional silencing and longevity protein Sir2 is an NAD-dependent histone deacetylase. *Nature* 2000;**403**:795–800.

Ishibashi H, Suzuki T, Suzuki S, Moriya T, Kaneko C, Takizawa T, Sunamori M, Handa M, Kondo T, Sasano H. Sex steroid hormone receptors in human thymoma. *J Clin Endocrinol Metab* 2003;**88**: 2309–2317.

Jacobsson B, Ladfors L, Milsom I. Advanced maternal age and adverse perinatal outcome. *Obstet Gynecol* 2004;**104**:727–733.

Jin J, Iakova P, Jiang Y, Medrano EE, Timchenko NA. The reduction of SIRT1 in livers of old mice leads to impaired body homeostasis and to inhibition of liver proliferation. *Hepatology* 2011;**54**: 989–998.

Johnson JA, Tough S; SOGC GENETICS COMMITTEE. Delayed child-bearing. *J Obstet Gynaecol Can* 2012;**34**:80–93.

Jolly M, Sebire N, Harris J, Robinson S, Regan L. The risks associated with pregnancy in women aged 35 years or older. *Hum Reprod* 2000;**15**:2433–2437.

Kaeberlein M, McVey M, Guarente L. The SIR2/3/4 complex and SIR2 alone promote longevity in *Saccharomyces cerevisiae* by two different mechanisms. *Genes Dev* 1999;**13**:2570–2580.

Kazgan N, Metukuri MR, Purushotham A, Lu J, Rao A, Lee S, Pratt-Hyatt M, Lickteig A, Csanaky IL, Zhao Y *et al*. Intestine-specific deletion of SIRT1 in mice impairs DCoH2-HNF-1alpha-FXR signaling and alters systemic bile acid homeostasis. *Gastroenterology* 2014; **146**:1006–1016.

Kelleher AM, Peng W, Pru JK, Pru CA, DeMayo FJ, Spencer TE. Forkhead box a2 (FOXA2) is essential for uterine function and fertility. *Proc Natl Acad Sci U S A* 2017;**114**:E1018–E1026.

Kennedy TG. Decidualization. In: Henry HL, Norman AW (eds). *Encyclopedia of Hormones*. New York: Academic Press, 2003,379–385.

Kim TH, Young SL, Sasaki T, Deaton JL, Schammel DP, Palomino WA, Jeong J-W, Lessey BA. Role of SIRT1 and progesterone resistance in normal and abnormal endometrium. *J Clin Endocrinol Metab* 2022;**107**:788–800.

Laisk T, Tsuiko O, Jatsenko T, Horak P, Otala M, Lahdenpera M, Lummaa V, Tuuri T, Salumets A, Tapanainen JS. Demographic and evolutionary trends in ovarian function and aging. *Hum Reprod Update* 2019;**25**:34–50.

Lamminpaa R, Vehvilainen-Julkunen K, Gissler M, Heinonen S. Preeclampsia complicated by advanced maternal age: a registry-based study on primiparous women in Finland 1997-2008. *BMC Pregnancy Childbirth* 2012;**12**:47.

Lee K, Jeong J, Kwak I, Yu CT, Lanske B, Soegiarto DW, Toftgard R, Tsai MJ, Tsai S, Lydon JP *et al*. Indian hedgehog is a major mediator of progesterone signaling in the mouse uterus. *Nat Genet* 2006;**38**: 1204–1209.

Lee KY, Jeong JW, Wang J, Ma L, Martin JF, Tsai SY, Lydon JP, DeMayo FJ. Bmp2 is critical for the murine uterine decidual response. *Mol Cell Biol* 2007;**27**:5468–5478.

Lee SH, Lee JH, Lee HY, Min KJ. Sirtuin signaling in cellular senescence and aging. *BMB Rep* 2019;**52**:24–34.

Li H, Rajendran GK, Liu N, Ware C, Rubin BP, Gu Y. SirT1 modulates the estrogen-insulin-like growth factor-1 signaling for postnatal development of mammary gland in mice. *Breast Cancer Res* 2007;**9**:R1.

Li Q, Kannan A, DeMayo FJ, Lydon JP, Cooke PS, Yamagishi H, Srivastava D, Bagchi MK, Bagchi IC. The antiproliferative action of progesterone in uterine epithelium is mediated by Hand2. *Science* 2011;**331**:912–916.

Long GY, Yang JY, Xu JJ, Ni YH, Zhou XL, Ma JY, Fu YC, Luo LL. SIRT1 knock-in mice preserve ovarian reserve resembling caloric restriction. *Gene* 2019;**686**:194–202.

Martin L, Das RM, Finn CA. The inhibition by progesterone of uterine epithelial proliferation in the mouse. *J Endocrinol* 1973;**57**: 549–554.

Matson BC, Pierce SL, Espenschied ST, Holle E, Sweatt IH, Davis ES, Tarran R, Young SL, Kohout TA, van Duin M *et al*. Adrenomedullin improves fertility and promotes pinopodes and cell junctions in the peri-implantation endometrium. *Biol Reprod* 2017;**97**:466–477.

McBurney MW, Yang X, Jardine K, Hixon M, Boekelheide K, Webb JR, Lansdorp PM, Lemieux M. The mammalian SIR2alpha protein has a role in embryogenesis and gametogenesis. *Mol Cell Biol* 2003; **23**:38–54.

Mills M, Rindfuss RR, McDonald P, te Velde E, Reproduction E; ESHRE Reproduction and Society Task Force. Why do people

postpone parenthood? Reasons and social policy incentives. *Hum Reprod Update* 2011;**17**:848–860.

Moore RL, Dai Y, Faller DV. Sirtuin 1 (SIRT1) and steroid hormone receptor activity in cancer. *J Endocrinol* 2012;**213**:37–48.

Nevoral J, Landsmann L, Stiavnicka M, Hosek P, Moravec J, Prokesova S, Rimnacova H, Koutna E, Klein P, Hoskova K *et al*. Epigenetic and non-epigenetic mode of SIRT1 action during oocyte meiosis progression. *J Anim Sci Biotechnol* 2019;**10**:67.

Norwitz ER. Defective implantation and placentation: laying the blueprint for pregnancy complications. *Reprod Biomed Online* 2006;**13**:591–599.

Paudel S, Liu B, Cummings MJ, Quinn KE, Bazer FW, Caron KM, Wang X. Temporal and spatial expression of adrenomedullin and its receptors in the porcine uterus and peri-implantation conceptuses. *Biol Reprod* 2021;**105**:876–891.

Ryall JG, Dell'Orso S, Derfoul A, Juan A, Zare H, Feng X, Clermont D, Koulnis M, Gutierrez-Cruz G, Fulco M *et al*. The NAD(+)-dependent SIRT1 deacetylase translates a metabolic switch into regulatory epigenetics in skeletal muscle stem cells. *Cell Stem Cell* 2015;**16**:171–183.

Salihu HM, Wilson RE, Alio AP, Kirby RS. Advanced maternal age and risk of antepartum and intrapartum stillbirth. *J Obstet Gynaecol Res* 2008;**34**:843–850.

Sansone AM, Hisrich BV, Young RB, Abel WF, Bowens Z, Blair BB, Funkhouser AT, Schammel DP, Green LJ, Lessey BA *et al*. Evaluation of BCL6 and SIRT1 as non-invasive diagnostic markers of endometriosis. *Curr Issues Mol Biol* 2021;**43**:1350–1360.

Sasaki T, Maier B, Bartke A, Scrable H. Progressive loss of SIRT1 with cell cycle withdrawal. *Aging Cell* 2006;**5**:413–422.

Satoh A, Brace CS, Rensing N, Cliften P, Wozniak DF, Herzog ED, Yamada KA, Imai S. Sirt1 extends life span and delays aging in mice through the regulation of Nk2 homeobox 1 in the DMH and LH. *Cell Metab* 2013;**18**:416–430.

Schug TT, Xu Q, Gao H, Peres-da-Silva A, Draper DW, Fessler MB, Purushotham A, Li X. Myeloid deletion of SIRT1 induces inflammatory signaling in response to environmental stress. *Mol Cell Biol* 2010;**30**:4712–4721.

Soyal SM, Mukherjee A, Lee KY, Li J, Li H, DeMayo FJ, Lydon JP. Cre-mediated recombination in cell lineages that express the progesterone receptor. *Genesis* 2005;**41**:58–66.

Stewart CL. The role of leukemia inhibitory factor (LIF) and other cytokines in regulating implantation in mammals. *Ann N Y Acad Sci* 1994;**734**:157–165.

Takano M, Lu Z, Goto T, Fusi L, Higham J, Francis J, Withey A, Hardt J, Cloke B, Stavropoulou AV *et al*. Transcriptional cross talk between the forkhead transcription factor forkhead box O1A and the progesterone receptor coordinates cell cycle regulation and differentiation in human endometrial stromal cells. *Mol Endocrinol* 2007;**21**:2334–2349.

Toiber D, Sebastian C, Mostoslavsky R. Characterization of nuclear sirtuins: molecular mechanisms and physiological relevance. *Handb Exp Pharmacol* 2011;**206**:189–224.

Vasquez YM, Mazur EC, Li X, Kommagani R, Jiang L, Chen R, Lanz RB, Kovanci E, Gibbons WE, DeMayo FJ. FOXO1 is required for binding of PR on IRF4, novel transcriptional regulator of endometrial stromal decidualization. *Mol Endocrinol* 2015;**29**:421–433.

Vasquez YM, Wang X, Wetendorf M, Franco HL, Mo Q, Wang T, Lanz RB, Young SL, Lessey BA, Spencer TE *et al*. FOXO1 regulates uterine epithelial integrity and progesterone receptor expression critical for embryo implantation. *PLoS Genet* 2018;**14**:e1007787.

Wang X, Li X, Wang T, Wu SP, Jeong JW, Kim TH, Young SL, Lessey BA, Lanz RB, Lydon JP *et al*. SOX17 regulates uterine epithelial-stromal cross-talk acting via a distal enhancer upstream of Ihh. *Nat Commun* 2018;**9**:4421.

Wang X, Wu SP, DeMayo FJ. Hormone dependent uterine epithelial-stromal communication for pregnancy support. *Placenta* 2017;**60**(Suppl 1):S20–S26.

Woods L, Morgan N, Zhao X, Dean W, Perez-Garcia V, Hemberger M. Epigenetic changes occur at decidualisation genes as a function of reproductive ageing in mice. *Development* 2020;**147**. https://doi.org/10.1038/s41467-017-00308-x

Woods L, Perez-Garcia V, Kieckbusch J, Wang X, DeMayo F, Colucci F, Hemberger M. Decidualisation and placentation defects are a major cause of age-related reproductive decline. *Nat Commun* 2017;**8**:352.

Yao Y, Li H, Gu Y, Davidson NE, Zhou Q. Inhibition of SIRT1 deacetylase suppresses estrogen receptor signaling. *Carcinogenesis* 2010;**31**:382–387.

Yi J, Luo J. SIRT1 and p53, effect on cancer, senescence and beyond. *Biochim Biophys Acta* 2010;**1804**:1684–1689.

Yoshizaki T, Milne JC, Imamura T, Schenk S, Sonoda N, Babendure JL, Lu JC, Smith JJ, Jirousek MR, Olefsky JM. SIRT1 exerts anti-inflammatory effects and improves insulin sensitivity in adipocytes. *Mol Cell Biol* 2009;**29**:1363–1374.

Zhu R, Wang SC, Sun C, Tao Y, Piao HL, Wang XQ, Du MR, Da-Jin L. Hyaluronan-CD44 interaction promotes growth of decidual stromal cells in human first-trimester pregnancy. *PLoS One* 2013;**8**:e74812.